

Uplift-driven diversification in the Hengduan Mountains, a temperate biodiversity hotspot

Yaowu Xing^{a,b,1} and Richard H. Ree^{a,c,1,2}

^aLife Sciences Section, Integrative Research Center, The Field Museum, Chicago, IL 60605; ^bKey Laboratory of Tropical Forest Ecology, Xishuangbanna Tropical Botanical Garden, Chinese Academy of Sciences, Yunnan 666303, China; and ^cNational Institute of Ecology, 1210 Geumgang-ro, Maseo-myeon, Seocheon-gun, Chungcheongnam-do, South Korea

Edited by Scott V. Edwards, Harvard University, Cambridge, MA, and approved February 27, 2017 (received for review September 26, 2016)

A common hypothesis for the rich biodiversity found in mountains is uplift-driven diversification—that orogeny creates conditions favoring rapid *in situ* speciation of resident lineages. We tested this hypothesis in the context of the Qinghai–Tibetan Plateau (QTP) and adjoining mountain ranges, using the phylogenetic and geographic histories of multiple groups of plants to infer the tempo (rate) and mode (colonization versus *in situ* diversification) of biotic assembly through time and across regions. We focused on the Hengduan Mountains region, which in comparison with the QTP and Himalayas was uplifted more recently (since the late Miocene) and is smaller in area and richer in species. Time-calibrated phylogenetic analyses show that about 8 million y ago the rate of *in situ* diversification increased in the Hengduan Mountains, significantly exceeding that in the geologically older QTP and Himalayas. By contrast, in the QTP and Himalayas during the same period the rate of *in situ* diversification remained relatively flat, with colonization dominating lineage accumulation. The Hengduan Mountains flora was thus assembled disproportionately by recent *in situ* diversification, temporally congruent with independent estimates of orogeny. This study shows quantitative evidence for uplift-driven diversification in this region, and more generally, tests the hypothesis by comparing the rate and mode of biotic assembly jointly across time and space. It thus complements the more prevalent method of examining endemic radiations individually and could be used as a template to augment such studies in other biodiversity hotspots.

biogeography | vascular plants | molecular clocks | dispersal | speciation

Central to understanding global patterns of biodiversity are considerations of biotic assembly: For a given region, when and how did resident species accumulate? Of primary interest is tempo (the rate of accumulation) and mode (the process, whether by colonization via dispersal or *in situ* lineage diversification). We wish to know how and why these vary in time and space.

For mountains, well-known for harboring a disproportionate fraction of terrestrial species, a common hypothesis is that of uplift-driven diversification—that orogeny creates conditions favoring *in situ* speciation of resident lineages (1–6). Among global biodiversity hotspots, the mountain ranges surrounding the Qinghai–Tibetan Plateau (QTP) are unusual and enigmatic: They harbor one of the world's richest temperate floras, and (unlike other hotspots) they are neither tropical nor Mediterranean in climate. Moreover, despite increasing interest from biogeographers, their biotic assembly remains poorly understood (3, 4, 7). The mountains form three distinct hotspots of biodiversity that respectively lie to the west, south, and east of the QTP's central high desert: the Central Asian mountains (Altai and Tianshan ranges), the Himalayas, and the Hengduan Mountains region (4) (Fig. 1). Of these, the richest in plant diversity is the Hengduan Mountains, with a vascular flora of about 12,000 species in an area of about 500,000 km² (8–10). In this study we seek to better understand the origins of this remarkable flora through the lens of historical biogeography. In particular,

was *in situ* diversification accelerated by uplift of the Hengduan Mountains?

The geological history of the QTP and its surrounding ranges is complex, and many details remain controversial, with different lines of evidence often yielding conflicting inferences. However, some points of consensus have emerged from recent syntheses (4, 11–13). One is that the central plateau was uplifted first, forming a “proto-QTP” as early as 40 Mya, with subsequent outward extensions by the early Miocene (11, 14). By the late Miocene, 8 to 10 Mya, all of the mountains surrounding the QTP to the south, west, and north had reached their current elevations (12, 15–17). By contrast, uplift of the Hengduan Mountains region, at the southeastern margin (Fig. 1), is generally believed to have been rapid and recent, occurring mainly between the late Miocene and late Pliocene (18–23).

The Hengduan Mountains are thus younger than the rest of the QTP and relatively small in area, but conspicuously rich in species. If floristic assembly tracks orogeny, this suggests an elevated tempo since the late Miocene, compared with adjacent regions, but what of mode? Either colonization, *in situ* diversification, or both processes must have been accelerated. In biogeographic studies of QTP-associated clades, the hypothesis of uplift-driven *in situ* diversification has been clearly favored over colonization, being commonly invoked to explain phylogenetic and phylogeographic divergences (e.g., refs. 24–27). However, conspicuously lacking from these studies are quantitative analyses that explicitly measure rates of diversification and colonization and compare them across regions and time (3, 4). Consequently, the idea that uplift-driven diversification has contributed

Significance

Why do so many species occur in mountains? A popular but little-tested hypothesis is that tectonic uplift creates environmental conditions (new habitats, dispersal barriers, etc.) that increase the rate at which resident species divide and evolve to form new ones. In China's Hengduan Mountains region, a biodiversity hotspot uplifted over the last 8 million years, this rate does in fact show a significant increase during that time, relative to the rate for adjacent older mountains, and to the rate of species immigration. The Hengduan Mountains flora is thus made up disproportionately of species that evolved within the region during its uplift, supporting the original hypothesis and helping to explain the prevalence of mountains as global biodiversity hotspots.

Author contributions: Y.X. and R.H.R. designed research, performed research, analyzed data, and wrote the paper.

The authors declare no conflict of interest.

This article is a PNAS Direct Submission.

Freely available online through the PNAS open access option.

¹Y.X. and R.H.R. contributed equally to this work.

²To whom correspondence should be addressed. Email: rree@fieldmuseum.org.

This article contains supporting information online at www.pnas.org/lookup/suppl/doi:10.1073/pnas.1616063114/-DCSupplemental.

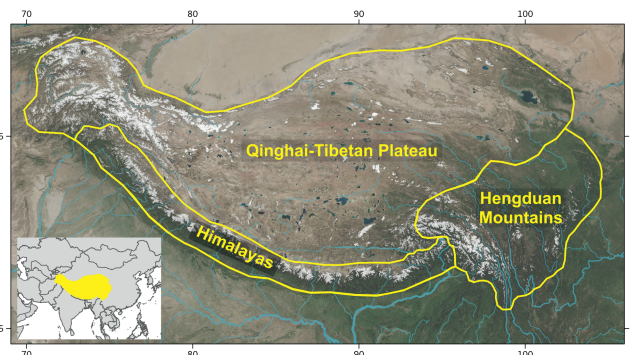


Fig. 1. Map of the Hengduan Mountains region in relation to the QTP and Himalayas.

disproportionately to floristic assembly in the Hengduan Mountains has yet to be rigorously tested.

In this study we used the evolutionary histories of multiple plant groups to study the floristic assembly of the Hengduan Mountains region, focusing on comparisons to adjacent regions, especially the Himalayas and other geologically older parts of the QTP (Fig. 1). We inferred regional rates of diversification and colonization through time from fossil-calibrated molecular chronograms and reconstructions of ancestral range and rates of lineage diversification, using data from 19 clades of vascular plants chosen for their potential to inform the biogeographic history of the Hengduan Mountains. Our primary aim was to discover the differences in tempo and mode of biotic assembly that help account for the remarkable diversity of the Hengduan flora.

Results

Contrasting Histories of Floristic Assembly. Reconstructed biogeographic histories of the selected clades reveal distinct patterns of floristic assembly across regions when plotted as the cumulative number of colonization and in situ speciation events through time (Fig. 2). We focus here on contrasting the Hengduan Mountains region with a combined Himalayas–QTP region to the west and temperate/boreal East Asia to the east (*Delimitation of Biogeographic Regions*). Given geological and paleontological evidence that the Hengduan Mountains are younger than the Himalayas–QTP, we expected to find that its flora was assembled more recently. Instead, we found surprisingly deep phylogenetic histories of Hengduan occupancy, with initial assembly of its flora predating that of the Himalayas–QTP. In more than 95% of the pseudoreplicated joint histories the earliest colonization event occurs by 64 Ma for the Hengduan Mountains and by 59 Ma for the Himalayas–QTP; in situ speciation begins later, starting by 34 Ma and 19 Ma, respectively. By contrast, in temperate/boreal East Asia, which was commonly reconstructed as the root ancestral area for clades, in situ speciation initially occurs by 155 Ma and colonization initially occurs by 60 Ma.

For all regions, species accumulation by each process is approximately exponential (log-linear) following initiation until about the last 8 Ma. During this earlier “constant” phase, assembly in both the Hengduan Mountains and Himalayas–QTP is dominated by colonization, whereas in temperate/boreal East Asia the dominant process is in situ speciation. Following this phase, the assembly dynamics of the Hengduan Mountains and Himalayas diverge considerably, with relatively little change in temperate/boreal East Asia. In the Hengduan Mountains, the cumulative number of in situ speciation events overtakes that of colonization around 8 Ma, and by the present the median number is 508 versus 335. In the Himalayas–QTP in situ speciation never overtakes colonization, and by the present the median

number of events is 192 versus 411. The relative contribution of in situ speciation to floristic assembly is thus $508/(508 + 335) = 0.603$ for the Hengduan Mountains, and $192/(192 + 411) = 0.318$ for the Himalayas–QTP. In other words, in situ speciation has contributed almost twice as much to the assembly of the Hengduan Mountains flora as it has to the Himalayas–QTP flora, especially since the late Miocene.

Regional Rates of in Situ Speciation and Dispersal Through Time. The rate of in situ speciation for the Hengduan Mountains region, in events per resident lineage per million years, increased almost twofold over the past 10 Ma, whereas for the Himalayas–QTP, it remained more or less constant (Fig. 3). Dispersal rates between the Hengduan Mountains and Himalayas–QTP increase gradually over the last 4 to 5 Ma, and sharply in the last 1 Ma. By contrast, dispersal from each region to temperate/boreal East Asia increases only slightly in the same time period (Fig. 4).

Shifts in Diversification Rate. Seven out of the 19 clades showed strong evidence (Bayes factor >15) for one or more shifts in diversification regime (Table 1). However, inspection of branch-specific evidence (the cumulative probability of occurring in the credible set of shift configurations, and the marginal odds ratio in favor of a shift) in light of ancestral-range reconstructions does not reveal any clear geographic patterns in the phylogenetic locations of regime shifts (SI Appendix, Fig. S2). That is, across clades, macroevolutionary jumps in diversification rate are not

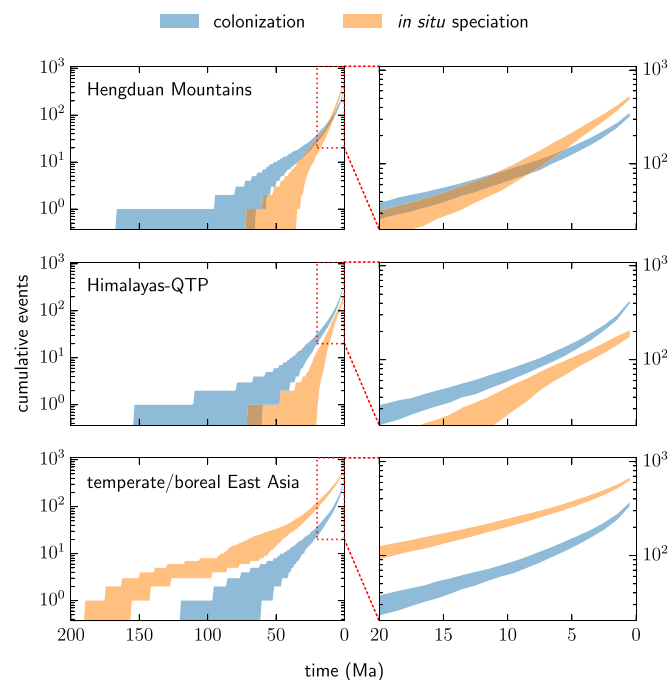


Fig. 2. Assembly of regional floras by colonization and in situ speciation events in 19 plant clades, inferred from ancestral-range reconstructions on time-calibrated molecular phylogenies. Shaded regions indicate the 5 to 95% quantile intervals for the cumulative number of events through time from 500 pseudoreplicated joint biogeographic histories designed to account for phylogenetic uncertainty (discussed in the text). Panels on the right focus on the last 20 Ma, in which differences in regional assembly are most apparent. In the Hengduan Mountains region, cumulative in situ speciation overtakes colonization about 8 Ma, whereas for the Himalayas–QTP colonization remains the dominant process. In situ speciation thus seems to have played a disproportionately large role in assembling the Hengduan Mountains flora since the late Miocene compared with the Himalayas–QTP, consistent with the theory of uplift-driven diversification in the Hengduan Mountains region.

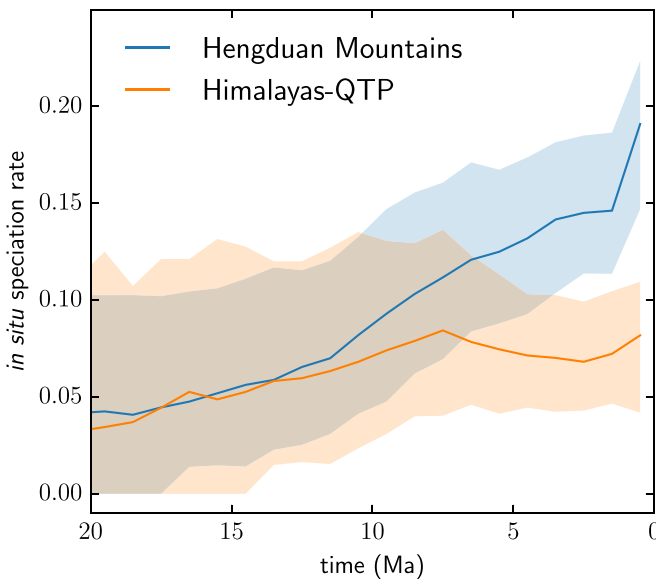


Fig. 3. Rolling estimates of in situ speciation rates through time for the Hengduan Mountains and Himalayas-QTP regions from inferred biogeographic histories of 19 plant clades. Lines indicate medians and shaded areas indicate 5 to 95% quantile intervals from 500 pseudoreplicated joint histories designed to account for phylogenetic uncertainty (discussed in the text). Regional rates begin to diverge about 8 Ma, with the Hengduan Mountains showing a striking increase in in situ speciation relative to the Himalayas-QTP.

obviously associated with the colonization or occupancy of any particular region.

A notable exception to this general pattern is *Rhododendron*, in which results from BAMM (Bayesian Analysis of Macroevolutionary Mixtures) and Lagrange suggest that in a window of about 9 to 15 Ma net diversification increased independently in two clades that each originated in the Hengduan region and are currently dominated by Hengduan species (Fig. 5). In *Saussurea*, an increase in net diversification is inferred about 1.7 Ma along the stem of a branch containing most of the clade's Hengduan species (SI Appendix, Fig. S2O). Similarly, in Delphineae, two separate increases are inferred in clades that are ancestrally Hengduan and together hold most of the Hengduan species; however, the times of these rate shifts (about 28 Ma and 37 Ma, respectively) predate the uplift of the Hengduan Mountains (SI Appendix, Fig. S2D). Finally, in *Isodon* and the *Ligularia-Cremanthodium-Parasenecio* complex, branch-specific measures show one increase in net diversification for each clade in the context of Hengduan ancestry about 7 and 5 Ma, respectively, but in both cases models with regime shifts are not supported by Bayes factors, and the Hengduan Mountains region is reconstructed as ancestral across most of the phylogeny, rendering the geographic context of the shift less informative.

Discussion

Our analysis quantifies the relative contributions of in situ lineage diversification and colonization to the assembly of one of the world's richest temperate floras, that of the Hengduan Mountains. We expected regional differences to reflect contrasting times of orogeny, in particular the prediction of the uplift-driven diversification hypothesis that in situ speciation increases with mountain-building activity. In this context, the late Miocene emerges as an important reference point, because previous studies of geology and paleontology indicate that the Hengduan Mountains achieved their current height only after this time, whereas the Himalayas and central QTP did so before

(4, 13, 15, 17, 21). Here, our phylogenetic inferences, which make no prior assumptions about the timing of geological events, show that after about 8 Ma the rate of in situ diversification increased in the Hengduan Mountains (Fig. 3), yielding a remarkable inflection point at which cumulative speciation overtakes colonization (Fig. 2). This indicates that the Hengduan Mountains flora has been assembled disproportionately by recent in situ diversification that coincides temporally with independent estimates of orogeny.

Rapid Himalayan orogeny during the early to middle Miocene (15, 21, 28) would predict a similar pulse of uplift-driven diversification, but none is evident whether the Himalayas are treated as part of the QTP (Fig. 3) or separately (SI Appendix, Fig. S4). It is possible that the Himalayas were uplifted more gradually; alternatively, the signal of such a pulse could be masked by the greater uncertainty associated with estimating clade ages and ancestral ranges in deeper time, and/or subsequent extinction and turnover in the affected lineages.

In a recent review, Renner (13) argued that numerous phylogenetic studies have misinterpreted the Earth sciences literature and incorrectly attributed relatively young (Miocene and later) estimates of lineage divergence to QTP uplift, and recommended that “Biogeographical discussions should also keep in mind expected differences in the biota of the TP and those in the Himalayas, the Kunlun range to the N, the Pamir and Karakoram to the W, and Hengduan Mountains to the E” (ref. 13, p. 7). Here, our focus on distinguishing the younger and more species-rich Hengduan Mountains region from the Himalayas-QTP is in the spirit of that advice, and our results suggest that at least some of the referenced cases of diversification could be more accurately interpreted as coincident with orogeny of the Hengduan

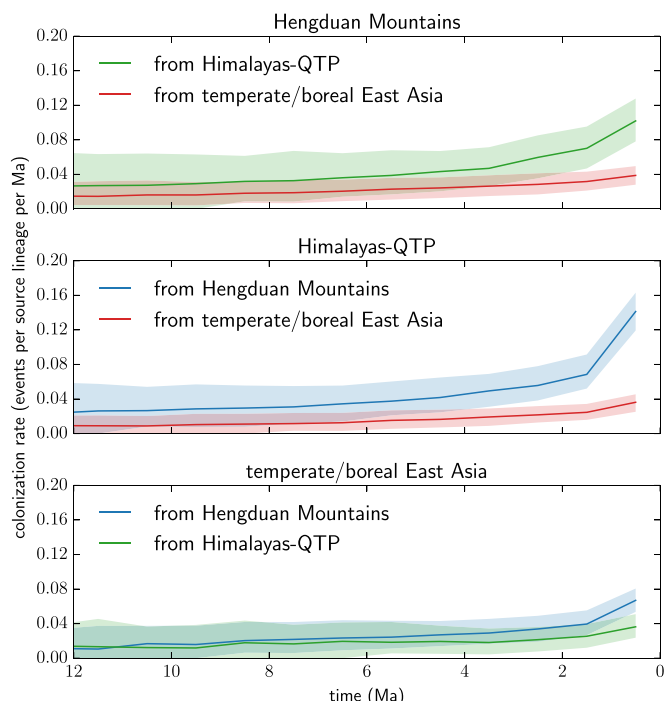


Fig. 4. Rolling estimates of colonization rates through time for the Hengduan Mountains, Himalayas-QTP, and temperate/boreal East Asia regions from inferred biogeographic histories of 19 plant clades. Lines indicate medians and shaded areas indicate 5 to 95% quantile intervals from 500 pseudoreplicated joint histories designed to account for phylogenetic uncertainty (discussed in the text). Dispersal between the Hengduan Mountains and Himalayas-QTP increases in the last 2 Ma relative to dispersal between either region and temperate/boreal East Asia.

Table 1. Bayes factor support for shifts in diversification in sampled clades, relative to the null hypothesis of no shifts

Clade	No. of regime shifts										
	1	2	3	4	5	6	7	8	9	10	11
<i>Acer</i>	31.76	71.62	26.07	5.59	1.05	0.12					
<i>Allium</i>	14.24	182.48	1,048.16	3,836.48	6,668.16	7,038.72	5,401.60	3,015.68	1,382.40	409.60	163.84
Clematidinae + Anemoninae	6.74	6.82	4.10	1.72	0.44	0.16	0.05				
<i>Cyananthus</i>	0.96	0.52	0.18	0.06	0.02	0.00					
<i>Delphineae</i>	377.43	5,871.71	6,889.71	4,316.57	1,872.00	566.86	137.14	36.57			
<i>Isodon</i>	8.18	8.60	5.23	2.23	0.94	0.19	0.06				
<i>Ligularia</i> – <i>Cremanthodium</i> – <i>Parasenecio</i> complex											
<i>Lilium</i> + <i>Nomocharis</i>	0.17	0.041	0.01								
<i>Meconopsis</i>	0.77	0.32	0.10	0.02	0.01						
Microsoroideae	3.83	4.37	2.79	1.19	0.38	0.11	0.07				
<i>Pinaceae</i>	40.78	29.36	10.15	2.17	0.34	0.05					
<i>Polygonaceae</i>	550.12	1,841.18	7,241.41	8,086.59	5,225.41	2,304.00	783.06	165.65			
Primulaceae	2.13	2.18	1.54	0.77	0.36	0.09	0.06	0.02			
<i>Rhodiola</i>	1.94	1.92	1.33	0.71	0.26	0.08	0.02				
<i>Rhododendron</i>	17.76	87.97	247.00	289.51	215.75	111.64	40.47	9.76	2.30		
<i>Rosa</i>	1.31	0.90	0.42	0.18	0.03	0.01					
<i>Saussurea</i>	7.30	20.21	21.68	13.56	6.26	2.01	0.35				
Saxifragaceae + Grossulariaceae	1.91	1.52	0.72	0.26	0.04	0.00					
<i>Thalictrum</i>	1.57	1.25	0.67	0.28	0.10	0.02	0.01				

Strong support (value >15) is indicated in bold.

region, not the older QTP. Indeed, several of the studies cited in Renner (13) are the original sources of molecular data for the clades analyzed here and include many Hengduan species. It thus seems important to emphasize that, despite precedent in the literature for considering the Hengduan Mountains to be simply part of a greater biogeographic region that includes the Himalayas and QTP (e.g., refs. 26, 27, 29, and 30), the Hengduan region actually has a very distinct history of assembly that reflects its younger age.

Why did *in situ* diversification in the Hengduan Mountains increase since the late Miocene, and, more specifically, to what extent was it driven by orogeny? Further studies are needed. One might look for contrasts between the Hengduan Mountains and adjacent regions in the evolution of ecological traits and environmental tolerances (e.g., ref. 31) across multiple clades. These may reveal, for example, the extent to which speciation within a region is associated with adaptive divergence and niche-filling, as opposed to nonadaptive processes such as genetic isolation and drift arising from dispersal limitation and topographic effects (vicariance, emergence of sky islands, etc.). These analyses would require denser and more fine-grained taxonomic and geographic sampling than was possible here, in addition to the requisite trait data. However, we suspect that evidence for common processes will prove elusive, because the proximate causes of diversification are likely to be idiosyncratic and involve a variety of contingencies and associated variables (e.g., refs. 32 and 33). For many clades, factors unrelated to uplift per se, such as biotic interactions, are almost certain to have played important roles (3, 13, 34). For example, in *Pedicularis* (Orobanchaceae) diversification of the many Hengduan species may have been facilitated by recurrent divergence in floral traits associated with pollinator sharing and reproductive interference (e.g., ref. 35), in combination with other mechanisms promoting population isolation, including uplift and associated aspects of landscape and resource heterogeneity.

A coarser-grained view is that diversification in the Hengduan region reflects a macroevolutionary response to the rapid expansion of moist temperate montane and alpine habitats in the late Miocene. At this level the effects of orogeny and climate change are not clearly separable, because they concur-

rently and jointly set a stage of ecological/evolutionary opportunity. During the early to middle Miocene, the southern QTP had already achieved its current elevation (15) and was covered by coniferous and deciduous-leaved forests (36, 37). As Hengduan uplift proceeded, falling temperatures would have driven the treeline lower, increasing the extent of shrublands, meadows, and scree slopes—habitats where most of the species in our dataset occur and would have diversified. Similar changes would also have occurred in the Himalayas and QTP, but in comparison with those areas moisture in the Hengduan region would have been abundant, because by then the summer monsoon was established, and the central QTP and Central Asian interior had aridified (13). This predicts that carrying capacities—and by extension, diversification potential—of the Hengduan region’s newly formed habitats were enhanced by greater summer rainfall.

Although not a driver of diversification per se, it is important to consider the effects of glaciation and climatic oscillations during the Pleistocene, and the possibility that our results can be explained, at least in part, by regional differences in extinction caused by these factors. In the Hengduan region, the north–south orientation of major valleys suggests that extinction was relatively low, because species would have been able to persist by migrating relatively unhindered toward southern ice-free areas during glacial cycles; as a result, the region’s history of *in situ* diversification would be better preserved in time-calibrated phylogenies, simply because fewer branches would have been “pruned” by extinction. By contrast, in the Himalayas–QTP, the east–west orientation of valleys would have inhibited southern displacement, leading to greater extinction. In this case, the pruning effect of extinction would yield lower estimates of *in situ* diversification during the Pleistocene.

This pattern is probably not due solely to differences in glacial extent. Numerous studies of species distributions (e.g., refs. 38 and 39) and phylogeography (e.g., refs. 40–43) support the idea that refugia occurred along the southeastern margin of the QTP as well as in areas further west and north, even at high elevation (e.g., refs. 44–46). This aligns with geological evidence that ice-free areas were present across the QTP and adjacent mountains throughout the Quaternary (47). It may be that

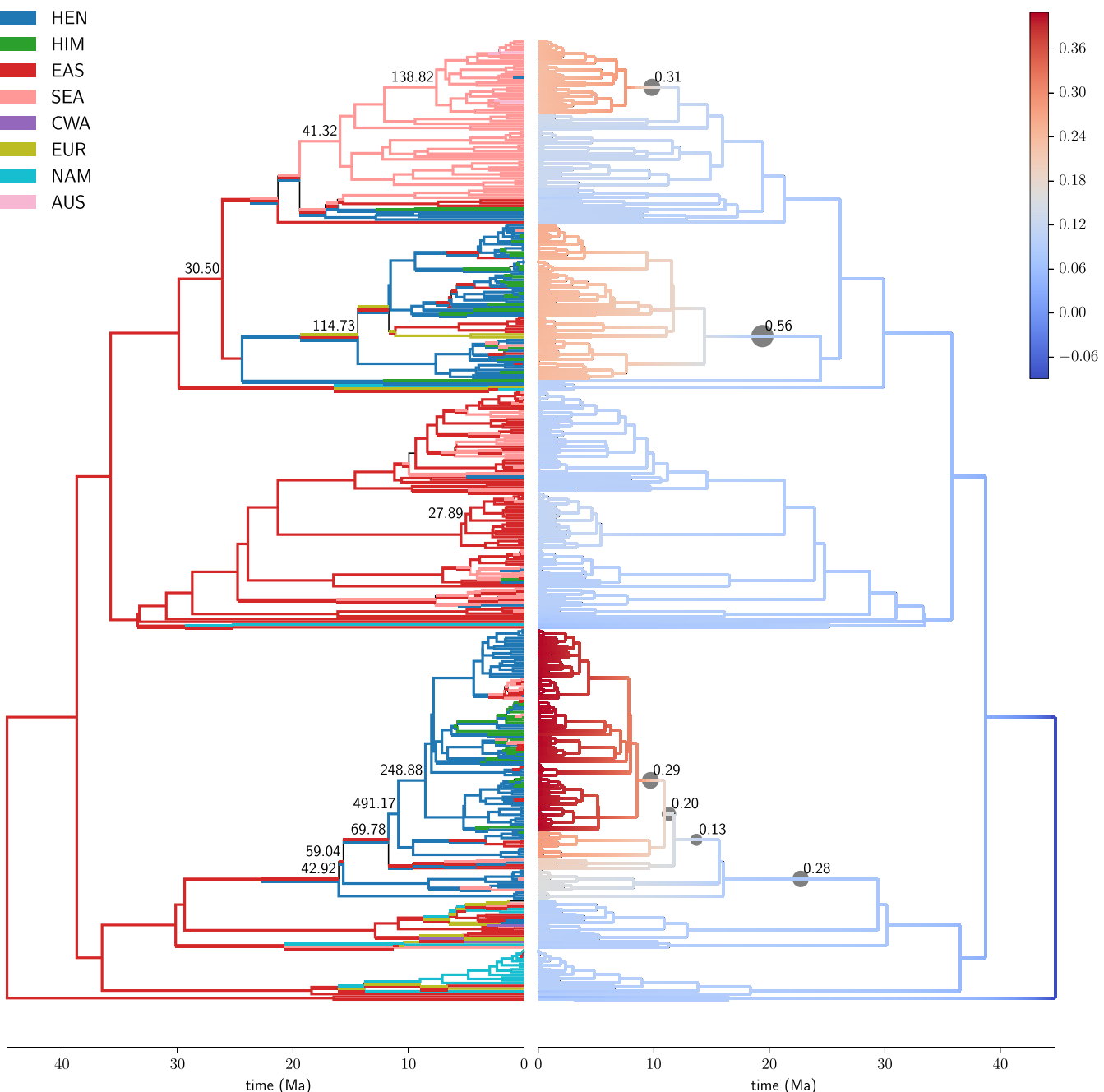


Fig. 5. Reconstructions of ancestral geographic range (Left) and net diversification rate (Right) on the maximum clade credibility tree, with branch lengths set to posterior means, for *Rhododendron*. Ancestral ranges are maximum-likelihood estimates at the start and end of each branch. Net diversification values are branch-segment means of the posterior distribution estimated by BAMM. Filled circles on the right indicate branches that appear in the 95% credible set of distinct shift configurations, with the size and label of a circle indicating the cumulative probability of the branch over all configurations in the credible set. On the left, the marginal odds ratio for a shift in diversification regime along a branch is drawn for branches where the ratio exceeds 20. Geographic regions are coded as follows: AUS, Australasia; CWA, central/western Asia; EAS, temperate-boreal East Asia; EUR, Europe; HEN, Hengduan Mountains; HIM, Himalayas–QTP; NAM, North America; and SEA, Southeast Asia. Hengduan species cluster primarily in two clades, both of which show evidence of ancestral shifts to higher diversification rate in the mid-to-late Miocene.

greater Pleistocene extinction in the Himalayas–QTP compared with the Hengduan region was driven as much (or more) by aridification as glaciation, because the former experienced reduced summer monsoon strength during interglacials (48).

These effects may be reflected in temporal patterns of dispersal between the Hengduan Mountains and Himalayas–QTP. The older age of the latter predicts that its flora should have been an early source of lineage dispersal to the younger Heng-

duan Mountains. However, we do not find any marked asymmetry in dispersal between these regions through the end of the Miocene; instead, rates in both directions are relatively low and increase only gradually until about 2 to 3 Ma, when both increase more sharply, but more so from the Hengduan Mountains to the Himalayas–QTP (Fig. 4). That is, in the Quaternary, the Hengduan Mountains seem to have acted as a biogeographic source, from which lineages buffered from extinction

colonized the relatively depauperate regions to the west and north.

Other than plants, the group that has received the most biogeographic scrutiny in relation to the QTP and adjacent regions is birds, which present similar patterns (49), notably that in the species-rich Hengduan Mountains region and adjacent forests of SE Asia, *in situ* diversification during and subsequent to the Miocene led to repeated colonization of the Himalayas and QTP (e.g., refs. 31, 50, and 51). In the Himalayas, the lack of *in situ* diversification of songbirds has been attributed to the filling of niches by preadapted colonizing lineages (52).

Among studies inferring biodiversity hotspot assembly from multiple clades, quantitative analyses of *in situ* diversification and/or colonization are still rare, and ours estimates rates of both processes through time and across regions. This comparative framework has allowed us to characterize, at a very basic level, changes in the tempo (rate) and mode (process) of biotic assembly in relation to independently inferred timelines of regional orogeny and climate change. By contrast, studies of other hotspots have tended to focus on single regions or biomes, and subsets of these dimensions (time, space, tempo, and mode). For example, the high species diversity in the California Floristic Province is associated with lower rates of extinction more than elevated speciation or immigration, using models in which rates of lineage birth, death, and movement are dependent on geographic occupancy but not time (53). Assembly of the Cerrado biome in Brazil has been characterized by recent (late Miocene onward) *in situ* adaptation of lineages to fire resistance (54), with some clades, especially in the campos rupestres highlands, showing evidence of endemic radiation [e.g., *Mimosa* (54, 55), *Calliandra* (56), and *Chamaecrista* (57)]. In the Páramo biome of the Andes, analyses of net diversification (but not immigration) yielded the highest average rate compared with eight other hotspots and appear driven more by Pleistocene climate oscillations than orogeny (58). Clearly, for the Hengduan Mountains, much remains to be studied about how patterns of assembly through time break down at a finer scale of particular biomes and habitats within the region.

The Andes, perhaps the world's richest mountain hotspot (2), are a compelling subject for comparison with the present results. The tropical montane/alpine habitats of the Andes are geographically isolated, whereas the temperate Hengduan region is embedded in a network of high mountains surrounding the QTP and proximate to cool high-latitude habitats. It thus stands to reason that dispersal figures prominently in Hengduan biotic assembly, compared with the Andes, in which endemic radiations are the more dominant pattern (e.g., refs. 5, 7, 34, 59, and 60).

Prevalence of dispersal is likely the main reason that we find little evidence of macroevolutionary jumps in diversification rate associated with Hengduan colonization in individual clades. In our phylogenies, clades tend not to be entirely endemic to the Hengduan Mountains or Himalayas–QTP; dispersal is common and reflects the fact that these regions are not defined by differences in biome but share broad physiographic similarities that presumably have facilitated biogeographic exchange. That is, dispersal between these regions should not necessarily require extensive ecophysiological adaptations that may be difficult to evolve (61), countering expectations of infrequent colonization events followed by endemic radiations (cf. ref. 60). For this reason our data are perhaps not well-suited for BAMM, which models diversification shifts as relatively rare events. Moreover, the link between dispersal events and shifts in diversification regime is further obscured by the inherent uncertainty associated with inferring their phylogenetic locations. The most appropriate interpretation may simply be that the signal of higher diversification in the Hengduan region is more or less diffuse across clades and emerges only when their biogeographic histories are consid-

ered jointly. This helps explain why previous analyses of single clades have not yielded the pattern inferred here.

The validity of our results hinges on the degree to which the data are representative of the focal regions (Hengduan Mountains and Himalayas–QTP). The clades we selected span a wide taxonomic range, and the species exhibit a diversity of growth forms, life histories, and habitat preferences. Taxon sampling, although incomplete, is not generally biased with respect to the focal regions (*SI Appendix, Table S1*) and therefore should not unduly affect inferences of the relative rates of assembly processes across regions. We also expect the phylogenetic distribution of unsampled species within each clade to be effectively random, which means that reconstructed phylogenies would tend to be missing more nodes—and thus inferred biogeographic events—closer to the present. In other words, the extent to which we have underestimated the frequencies of those events is likely greater in the Pliocene and Quaternary than in the Miocene and earlier.

Another potential source of error is in the demarcation of discrete areas as required for biogeographic analysis. Although the QTP, Himalayas, and Hengduan Mountains may have broadly distinct orogenic histories, this does not translate into clearly defined borders, and to the extent such borders existed they surely would have shifted through time, leading to ambiguity in the present. Our definitions of these areas (Fig. 1) are thus necessarily somewhat subjective and represent our best attempts to capture the essential elements of this complex system. That being said, our results are robust to the treatment of the Himalayas and QTP as a single biogeographic area; an analysis of recoded species range data treating them as separate areas yielded the same signature of uplift-driven Hengduan diversification (*SI Appendix, Additional Analyses of Biotic Assembly* and Figs. S3–S5).

Materials and Methods

Clade Selection and Phylogeny Reconstruction. Our criteria were that each clade (*i*) included a substantial number of species that occur in the Hengduan Mountains, as well as their closest known relatives in other biogeographic regions, (*ii*) had sufficient molecular data available to infer a phylogeny that was broadly representative of the clade's taxonomic diversity and geographic range, and (*iii*) had fossil data suitable for molecular clock calibration or secondary calibrations inferred from fossil dated phylogenies. We found 19 clades—17 of angiosperms and one each of gymnosperms (Pinaceae) and ferns (Microsorioideae)—that met these criteria. The combined taxon sample included 4,668 ingroup species, of which 930 occur in the Hengduan Mountains region, 703 in the Himalayas–QTP, and 1,045 in the remainder of temperate/boreal East Asia (*Delimitation of Biogeographic Regions*). About 370 species are shared between the Hengduan Mountains and Himalayas–QTP regions. Across clades, the proportion of species sampled ranged from 20 to 97% globally and 26 to 94% for the Hengduan Mountains region (*SI Appendix, Table S1*).

For each clade, we assembled molecular sequence alignments (*Dataset S1*) and fossil calibration data and used relaxed molecular clock models implemented in BEAST (Bayesian Evolutionary Analysis Sampling Trees) (62, 63) to generate a Bayesian posterior sample of time-calibrated phylogenies and the associated maximum-clade-credibility tree (*SI Appendix*).

Inference of Range Evolution and Lineage Diversification.

Delimitation of biogeographic regions. We delimited 11 biogeographic regions (*SI Appendix, Fig. S1*) and scored the range of each sampled species as its presence or absence in these regions based on floras, online databases, and published datasets (*SI Appendix* and *Dataset S2*). Delimitations reflected our need to accommodate the global distributions of the selected clades and the granularity of available species range data, and most importantly to focus on distinguishing the Hengduan Mountains region from adjacent, geologically older parts of the QTP, especially the Himalayas (Fig. 1).

The Hengduan Mountains region, following Boufford (8), is bounded to the west by the Yarlung Tsangpo River in eastern Xizang (Tibet), to the northwest by the high plateau in Qinghai, to the north by the Tao River in southern Gansu, to the east by the Sichuan Basin, and to the south by subtropical forests and the Yunnan–Guizhou Plateau (Fig. 1). We delimited the complementary “Himalayas–QTP” region as including the plateau itself, the Himalayas to the south, the Kunlun Mountains to the north, and the

Qilian Mountains to the northeast. The distinct geological histories of the Himalayas and QTP argue against their treatment as a single unit for biogeographic analysis; however, the granularity of available data on species ranges made it difficult to differentiate between them. We attempted to do so, with no effect on outcomes (*SI Appendix, Additional Analyses of Biotic Assembly and Figs. S3–S5*), but we are most confident with analyses based on the combined delimitation, which effectively serves the purpose of contrasting with the Hengduan region.

The other regions we delimited are temperate/boreal East Asia (the eastern boreal part of Russia and temperate regions of East Asia, including Japan and Taiwan), central/western Asia (including the Xinjiang Uyghur Autonomous Region to the north of the Kunlun Range), southeast Asia (including tropical regions of China, Malesia, and Papuasia), Australasia (Australia, New Zealand, and the southwestern Pacific), India (south of the Himalayas, including Sri Lanka), Africa, Europe, North America, and South America (south of the Panama Canal).

Ancestral range reconstruction. We estimated ancestral geographic ranges for all ingroups using a dispersal-extinction-cladogenesis model in Lagrange (64, 65) in which dispersal was allowed based on spatial adjacency (*SI Appendix, Fig. S1*) and the maximum range size was set to 3. We explicitly avoided placing any temporal constraints on dispersal, so that biogeographic inferences were independent of prior beliefs about the ages of the Hengduan Mountains or Himalayas–QTP regions. For each ingroup we inferred a distribution of biogeographic histories to account for phylogenetic uncertainty. A single history was generated in three steps. First, a chronogram was randomly sampled from the clade's Bayesian posterior distribution. Second, the maximum-likelihood set of ancestral ranges (geographic speciation scenarios) at internal nodes was estimated using Lagrange. Third, parsimonious sequences of dispersal and local extinction events were randomly interpolated along branches having different ancestral and descendant ranges. This procedure yielded a complete chronology of biogeographic events (i.e., where and when ancestral lineages moved and underwent speciation and local extinction). To account for phylogenetic uncertainty, one history was generated for each of 500 chronograms sampled from the posterior for each clade.

Regional assembly processes through time. We focused our analysis on the dynamics of the Hengduan Mountains region in comparison with the Himalayas–QTP and temperate East Asia. Our objective was to estimate, for each region, rates of in situ diversification and colonization and their cumulative contributions to biotic assembly through time, while accounting for phylogenetic uncertainty. Taking the biogeographic histories of clades from the ancestral-range analysis, we generated 500 pseudoreplicated joint histories—sets of one history drawn randomly from each clade's pool without replacement. From each joint history we extracted the chronology of

in situ speciation, colonization, and local extinction events affecting the Hengduan Mountains, Himalayas–QTP, and temperate/boreal East Asia, and binned them into 1-My periods. This allowed region-specific estimates of assembly processes through time. We calculated rolling estimates of per capita in situ speciation rates as $\lambda(t) = s(t)/n(t - 1)$, where $s(t)$ is the number of in situ speciation events inferred in a region in a 1-My period t and $n(t - 1)$ is the number of inferred lineages in the region in the previous period (the cumulative sum of in situ speciation and colonization minus local extinction). We also calculated rolling per capita rates of colonization between regions as $d_{ij}(t) = c_{ij}(t)/n_i(t - 1)$, where $c_{ij}(t)$ is the number of inferred colonization events of area j from area i . For all estimates, confidence intervals (5 to 95% quantiles) were calculated from the pseudoreplicated joint histories. Our results thus do not condition on any particular tree topologies or branch lengths and reflect the levels of clade support, and confidence in divergence times, provided by the sequence data.

Geography-independent rates of diversification. To complement the regional-process analysis and to better understand heterogeneity in rates of lineage diversification independently of geography, we generated Bayesian inferences of diversification rate for each clade's maximum-clade-credibility tree, with posterior mean branch lengths, using BAMM version 2.5 and the BAMMtools R package (66). BAMM uses Markov chain Monte Carlo procedures to jointly estimate the number, parameters, and locations of distinct macroevolutionary regimes (rates of lineage birth and death, possibly time-dependent) on a phylogenetic tree. It can account statistically for incomplete taxon sampling, so we assigned sampling fractions at the finest level of taxonomic resolution possible (*SI Appendix*). Priors for speciation and extinction were set empirically using the `setBAMMPriors` function. For all clades smaller than 500 species we set the geometric prior on the expected number of regime shifts to 1, as recommended in the BAMM documentation; for larger clades we also tested a prior of 10 expected shifts. We ran each BAMM Markov chain Monte Carlo analysis for 10 million generations with a sampling frequency of 1/1,000 and assessed convergence by visually inspecting plots of the likelihood trace and calculating the effective sample size after discarding the first 10% of the run as burn-in. For each clade, we calculated Bayes factors for the distinct numbers of regime shifts sampled, marginal odds ratios (relative evidence in favor of a shift) for individual branches, and the 95% credible set of distinct shift configurations.

ACKNOWLEDGMENTS. We thank D. Boufford and three anonymous reviewers for valuable comments on previous drafts. This work was supported by a Boyd Postdoctoral Fellowship at the Field Museum, Swiss Advanced Postdoc.Mobility Fellowship P300P3_158528, the Pioneer Hundred Talents Program of the Chinese Academy of Sciences (Y.X.), and NSF Grant DEB-1119098 (to R.H.R.).

1. Hoorn C, Mosbrugger V, Mulch A, Antonelli A (2013) Biodiversity from mountain building. *Nat Geosci* 6:154–154.
2. Hughes CE (2016) The tropical Andean plant diversity powerhouse. *New Phytol* 210:1152–1154.
3. Wen J, Zhang JQ, Nie ZL, Zhong Y, Sun H (2014) Evolutionary diversifications of plants on the Qinghai-Tibetan Plateau. *Front Genet* 5:1–16.
4. Favre A, et al. (2015) The role of the uplift of the Qinghai-Tibetan Plateau for the evolution of Tibetan biotas. *Biol Rev* 90:236–253.
5. Lagomarsino LP, Condamine FL, Antonelli A, Mulch A, Davis CC (2016) The abiotic and biotic drivers of rapid diversification in Andean bellflowers (Campanulaceae). *New Phytol* 210:1430–1442.
6. Schwery O, et al. (2015) As old as the mountains: The radiations of the Ericaceae. *New Phytol* 207:355–367.
7. Hughes CE, Atchison GW (2015) The ubiquity of alpine plant radiations: From the Andes to the Hengduan Mountains. *New Phytol* 207:275–282.
8. Boufford D (2014) Biodiversity hotspot: China's Hengduan Mountains. *Arnoldia* 72:24–35.
9. Li XW, Li J (1993) A preliminary floristic study on the seed plants from the region of Hengduan Mountain. *Yunnan-zhiwu-yanjiu* 15:217–231.
10. Wu ZY (1988) Hengduan mountain flora and her significance. *J Jpn Bot* 63: 297–311.
11. Wang C, et al. (2014) Outward-growth of the Tibetan Plateau during the Cenozoic: A review. *Tectonophysics* 621:1–43.
12. Deng T, Ding L (2015) Paleoaltimetry reconstructions of the Tibetan Plateau: Progress and contradictions. *Natl Sci Rev* 2:417–437.
13. Renner SS (2016) Available data point to a 4-km-high Tibetan Plateau by 40 Ma but 100 molecular-clock papers have linked supposed recent uplift to young node ages. *J Biogeogr* 43:1479–1487.
14. Rowley DB, Currie BS (2006) Palaeo-altimetry of the late Eocene to Miocene Lunpola basin, central Tibet. *Nature* 439:677–681.
15. Spicer RA, et al. (2003) Constant elevation of southern Tibet over the past 15 million years. *Nature* 421:622–624.
16. Fang X, et al. (2005) Magnetostratigraphy of the late Cenozoic Laojunmiao anticline in the northern Qilian Mountains and its implications for the northern Tibetan Plateau uplift. *Sci China Ser D* 48:1040–1051.
17. Wang Y, et al. (2012) Cenozoic uplift of the Tibetan Plateau: Evidence from the tectonic-sedimentary evolution of the western Qaidam Basin. *Geosci Front* 3:175–187.
18. Kirby E, et al. (2002) Late Cenozoic evolution of the eastern margin of the Tibetan Plateau: Inferences from 40Ar/39Ar and (U-Th)/He thermochronology. *Tectonics* 21: 1–20.
19. Clark MK, et al. (2005) Late Cenozoic uplift of southeastern Tibet. *Geology* 33:525–528.
20. Wang E, et al. (2012) Two-phase growth of high topography in eastern Tibet during the Cenozoic. *Nat Geosci* 5:640–645.
21. Wang P, et al. (2014) Tectonic control of Yarlung Tsangpo Gorge revealed by a buried canyon in Southern Tibet. *Science* 346:978–981.
22. Meng K, Wang E, Wang G (2016) Uplift of the Emei Shan, western Sichuan Basin: Implication for eastward propagation of the Tibetan Plateau in Early Miocene. *J Asian Earth Sci* 115:29–39.
23. Sun BN, et al. (2011) Reconstructing Neogene vegetation and climates to infer tectonic uplift in western Yunnan, China. *Palaeogeogr, Palaeoclimatol, Palaeoecol* 304:328–336.
24. Liu JQ, Wang YJ, Wang AL, Hideaki O, Abbott RJ (2006) Radiation and diversification within the *Ligularia*–*Cremanthodium*–*Parasenecio* complex (Asteraceae) triggered by uplift of the Qinghai-Tibetan Plateau. *Mol Phylogenet Evol* 38:31–49.
25. Wang Y, Susanna A, von Raab-Straube E, Milne R, Liu J (2009) Island-like radiation of *Saussurea* (Asteraceae: Cardueae) triggered by uplifts of the Qinghai-Tibetan Plateau. *Biol J Linn Soc* 97:893–903.
26. Zhang JQ, Meng SY, Allen GA, Wen J, Rao GY (2014) Rapid radiation and dispersal out of the Qinghai-Tibetan Plateau of an alpine plant lineage *Rhodiola* (Crassulaceae). *Mol Phylogenet Evol* 77:147–158.
27. Gao YD, Harris AJ, Zhou SD, He XJ (2013) Evolutionary events in *Lilium* (including *Nomocharis*, Liliaceae) are temporally correlated with orogenies of the Q–T plateau and the Hengduan Mountains. *Mol Phylogenet Evol* 68:443–460.

28. Searle MP (2011) Geological evolution of the Karakoram Ranges. *Ital J Geosci* 130:147–159.
29. Nie ZL, et al. (2013) Molecular phylogeny of *Anaphalis* (Asteraceae, Gnaphalieae) with biogeographic implications in the Northern Hemisphere. *J Plant Res* 126:17–32.
30. Matuszak S, Muellner-Riehl AN, Sun H, Favre A (2016) Dispersal routes between biodiversity hotspots in Asia: The case of the mountain genus *Tripterospermum* (Gentianinae, Gentianaceae) and its close relatives. *J Biogeogr* 43:580–590.
31. Liu Y, et al. (2016) Sino-Himalayan mountains act as cradles of diversity and immigration centres in the diversification of parrotbills (Paradoxornithidae). *J Biogeogr* 43:1488–1501.
32. Donoghue MJ, Sanderson MJ (2015) Confluence, synnovation, and depauperons in plant diversification. *New Phytol* 207:260–274.
33. Bouchenak-Khelladi Y, Onstein RE, Xing Y, Schwery O, Linder HP (2015) On the complexity of triggering evolutionary radiations. *New Phytol* 207:313–326.
34. Luebert F, Weigend M (2014) Phylogenetic insights into Andean plant diversification. *Evol Popul Genet* 2:27.
35. Eaton DAR, Fenster CB, Hereford J, Huang SQ, Ree RH (2012) Floral diversity and community structure in *Pedicularis* (Orobanchaceae). *Ecology* 93:S182–S194.
36. Sun J, et al. (2014) Palynological evidence for the latest Oligocene-early Miocene paleoelevation estimate in the Lunpola Basin, central Tibet. *Palaeogeogr, Palaeoclimatol, Palaeoecol* 399:21–30.
37. Li H, Guo S (1976) The Miocene flora Namling of Xizang. *Gu sheng wu xue bao* 15: 7–17.
38. Srinivasan U, Tammar K, Ramakrishnan U (2014) Past climate and species ecology drive nested species richness patterns along an east-west axis in the Himalaya: Nestedness in Himalayan fauna. *Global Ecol Biogeogr* 23:52–60.
39. López-Pujol J, Zhang FM, Sun HQ, Ying TS, Ge S (2011) Centres of plant endemism in China: Places for survival or for speciation? *J Biogeogr* 38:1267–1280.
40. Cun YZ, Wang XQ (2010) Plant recolonization in the Himalaya from the southeastern Qinghai-Tibetan Plateau: Geographical isolation contributed to high population differentiation. *Mol Phylogenet Evol* 56:972–982.
41. Wang B, Mao JF, Gao J, Zhao W, Wang XR (2011) Colonization of the Tibetan Plateau by the homoploid hybrid pine *Pinus densata*. *Mol Evol* 20:3796–3811.
42. Lei F, Qu Y, Song G (2014) Species diversification and phylogeographical patterns of birds in response to the uplift of the Qinghai-Tibet Plateau and Quaternary glaciations. *Curr Zool* 60:149–161.
43. Meng L, et al. (2015) Refugial isolation and range expansions drive the genetic structure of *Oxyria sinensis* (Polygonaceae) in the Himalaya-Hengduan Mountains. *Sci Rep* 5:10396.
44. Wang L, et al. (2009) History and evolution of alpine plants endemic to the Qinghai-Tibetan Plateau: *Aconitum gymnanthrum* (Ranunculaceae). *Mol Evol* 18:709–721.
45. Sun YS, Ikeda H, Wang YJ, Liu JQ (2010) Phylogeography of *Potentilla fruticosa* (Rosaceae) in the Qinghai-Tibetan Plateau revisited: A reappraisal and new insights. *Plant Ecol Divers* 3:249–257.
46. Opgenoorth L, et al. (2010) Tree endurance on the Tibetan Plateau marks the world's highest known tree line of the Last Glacial Maximum. *New Phytol* 185: 332–342.
47. Owen LA, Dortch JM (2014) Nature and timing of Quaternary glaciation in the Himalayan-Tibetan orogen. *Quaternary Sci Rev* 88:14–54.
48. Owen LA, Caffee MW, Finkel RC, Seong YB (2008) Quaternary glaciation of the Himalayan-Tibetan orogen. *J Quaternary Sci* 23:513–531.
49. Päckert M, Martens J, Sun YH, Tietze DT (2015) Evolutionary history of passerine birds (Aves: Passeriformes) from the Qinghai-Tibetan plateau: From a pre-Quaternary perspective to an integrative biodiversity assessment. *J Ornithol* 156:355–365.
50. Tietze DT, Päckert M, Martens J, Lehmann H, Sun YH (2013) Complete phylogeny and historical biogeography of true rosefinches (Aves: *Carpodacus*). *Zool J Linn Soc* 169:215–234.
51. Johansson US, et al. (2007) Build-up of the Himalayan avifauna through immigration: A biogeographical analysis of the *Phylloscopus* and *Seicercus* warblers. *Evolution* 61:324–333.
52. Price TD, et al. (2014) Niche filling slows the diversification of Himalayan songbirds. *Nature* 509:222–225.
53. Lancaster LT, Kay KM (2013) Origin and diversification of the California flora: Re-examining classic hypotheses with molecular phylogenies. *Evolution* 67:1041–1054.
54. Simon MF, et al. (2009) Recent assembly of the Cerrado, a neotropical plant diversity hotspot, by *in situ* evolution of adaptations to fire. *Proc Natl Acad Sci USA* 106:20359–20364.
55. Koenen EJM, et al. (2013) Exploring the tempo of species diversification in legumes. *S Afr J Bot* 89:19–30.
56. de Souza ER, et al. (2013) Phylogeny of *Calliandra* (Leguminosae: Mimosoideae) based on nuclear and plastid molecular markers. *Taxon* 62:1200–1219.
57. Rando JG, et al. (2015) Phylogeny of *Chamaecrista* ser. *Coriacea* (Leguminosae) unveils a lineage recently diversified in Brazilian campo rupestre vegetation. *Int J Plant Sci* 177:3–17.
58. Madriñán S, Cortés AJ, Richardson JE (2013) Páramo is the world's fastest evolving and coolest biodiversity hotspot. *Front Genet* 4:192.
59. Pennington RT, et al. (2010) Contrasting plant diversification histories within the Andean biodiversity hotspot. *Proc Natl Acad Sci USA* 107:13783–13787.
60. Hughes C, Eastwood R (2006) Island radiation on a continental scale: Exceptional rates of plant diversification after uplift of the Andes. *Proc Natl Acad Sci USA* 103:10334–10339.
61. Donoghue MJ, Edwards EJ (2014) Biome shifts and niche evolution in plants. *Annu Rev Ecol Evol Systemat* 45:547–572.
62. Drummond AJ, Suchard MA, Xie D, Rambaut A (2012) Bayesian phylogenetics with BEAUti and the BEAST 1.7. *Molecular Biology And Evolution* 29:1969–1973.
63. Bouckaert R, et al. (2014) BEAST 2: A software platform for Bayesian evolutionary analysis. *PLoS Comput Biol* 10:e1003537.
64. Ree RH, Moore BR, Webb CO, Donoghue MJ (2005) A likelihood framework for inferring the evolution of geographic range on phylogenetic trees. *Evolution* 59:2299–2311.
65. Ree RH, Smith SA (2008) Maximum likelihood inference of geographic range evolution by dispersal, local extinction, and cladogenesis. *Syst Biol* 57:4–14.
66. Rabosky DL (2014) Automatic detection of key innovations, rate shifts, and diversity-dependence on phylogenetic trees. *PLoS One* 9:e89543.

1 Supporting Information

2 Molecular dating: calibrations and topological constraints

3 Below we list and explain the node age constraints used in calibrating the divergence-time analyses in BEAST. For
4 each analysis, the ingroup is the taxon for which divergence times and ancestral geographic ranges were
5 reconstructed; the “outgroup scope” is the least-inclusive taxon containing the ingroup and outgroup taxa. Included
6 in the list are fossil-calibrated “backbone” analyses that we ran to derive secondary calibrations for some ingroups. A
7 spreadsheet containing taxon-by-gene tables of Genbank accession numbers for all analyses is available as Dataset
8 S1.

9 Unless otherwise noted, the age ranges are the bounds of a uniform prior distribution, and the nodes in
10 question were topologically constrained to be monophyletic. Wherever possible, we used fossils to set the minimum
11 (lower) bounds for these priors. For eudicot angiosperm nodes, we set the upper (older) bound to 125 Ma, the age of
12 the earliest eudicot fossil [29], if no other evidence was available for a younger constraint.

13 Ingroup: *Acer*; outgroup scope: Sapindaceae

- 14 1. **Stem age of *Dipteronia*:** 60–125 Ma. The lower bound is based on the earliest fossil of *Dipteronia*, winged
15 fruits from the Paleocene of North America [46].
- 16 2. **Crown age of *Acer*:** 47.8–125 Ma. *Acer* has a rich fossil record, dating to at least the Paleocene [42, 67]. We
17 based the lower bound on the crown age on the first fossil samaras assignable to *Acer* section *Acer*, from the
18 latest Early Eocene of North America [67].

19 Ingroup: *Allium*; outgroup scope: Amaryllidaceae

- 20 There are no reliable fossils for Amaryllidaceae, so we used secondary calibrations from a fossil-calibrated study of
21 the containing order Asparagales [14].
 - 22 1. **Root (crown age of Amaryllidaceae):** 42.0–61.7 Ma. The bounds equal the 95% highest posterior density
23 (HPD) interval of the crown age of Amaryllidaceae from [14].
 - 24 2. **Crown age of Allioideae:** 27.8–44.5 Ma. The bounds equal the 95% HPD interval of the crown age of
25 Allioideae from [14].

26 Ingroups: Clematidinae+Anemoninae, Delphineae, and *Thalictrum*; outgroup scope: Ranunculaceae

- 27 Divergence times for these ingroups were estimated in separate analyses that shared a common set of calibrations.
 - 28 1. **Root (crown age of Ranunculaceae):** 93.9–125 Ma. The lower bound is based on pollen of *Cretacaeisporites*
29 *scabratus* from the Cretaceous (probably Late Cenomanian) of Gabon [64].

- 30 2. **Stem age of *Actaea*:** 56.8–125 Ma. The lower bound is based on fossil fruits (*Paleoactaea nagelii*) from the
31 late Paleocene of North Dakota [50].
- 32 3. **Stem age of *Clematis*:** 23–125 Ma. The lower bound is based on fossil fruits of the genus from the Oligocene
33 of Germany [66].
- 34 4. **Stem age of *Caltha*:** 70.6–125 Ma. The lower bound is based on fossil *Eocaltha zoophilia* from the
35 Campanian of Mexico [53].
- 36 5. **Stem age of *Ranunculus*:** 23–125 Ma. The lower bound is based on fossil fruits of the genus from the
37 Oligocene [41].

38 **Ingroup: *Cyananthus*; outgroup scope: Campanulaceae**

- 39 1. **Root (crown age of Campanulaceae):** 62–90 Ma. The bounds equal the 95% HPD interval of the crown age
40 of Campanulaceae inferred in [40].
- 41 2. **Stem age of the most recent common ancestor of *Campanula pyramidalis* and *C. carpatica*:** 16.5–62 Ma.
42 The bounds are based on fossils of *C. palaeopyramidalis* [34] which were assigned to *C. pyramidalis* in [12].

43 **Ingroup: *Isodon*; outgroup scope: Lamiaceae**

- 44 The following constraints are based on 95% HPD intervals for node ages from the fossil-calibrated study by Yu *et al.*
45 [71].
- 46 1. **Stem age of *Isodon*:** 17.03–39.84 Ma.
- 47 2. **Crown age of *Isodon*:** 14.66–26.44 Ma.

48 **Backbone: Asteraceae; outgroup scope: Asterales**

- 49 This analysis was run to derive secondary calibrations for the *Ligularia-Cremanthodium-Parasenecio* complex and
50 *Saussurea*, both of which lack fossils.
- 51 1. **Crown age of Asteraceae:** 72.1–125 Ma. The lower bound is based on Cretaceous pollen of *Tubulifloridites*
52 *lilliei* type A, which was used to constrain of the divergence time of *Barnadesia* and *Dasyphyllum* in [5].
- 53 2. **Stem age of Asteraceae excluding Barnadesieae and Famatinianthus:** 47.5–125 Ma. The lower bound is
54 based on *Raiguernrayum cura*, an exceptionally well-preserved capitulecence from the 47.5 Ma Huitrera
55 Formation in Argentina [2, 4] that shares a mosaic of morphological characters with modern groups such as
56 Stifttieae, Mutisioideae sensu lato, and Carduoideae.

- 57 3. **Stem age of Mutisieae:** 28.5–125 Ma. The lower bound is based on the earliest unequivocal fossil pollen for
58 Mutisieae, *Mutisiapollis patersonii*, from the early Oligocene of Australia [39]. The pollen is similar to that of
59 some extant species in *Chaetanthera* and *Mutisia*, however, it cannot be clearly placed within any extant genus.
- 60 4. **Stem age of Nassauvieae:** 16.0–125 Ma. The lower bound was set by the earliest fossil pollen of Nassauvieae,
61 *Huanilipollis cabrerii*, from early Miocene sediments in South America [2, 3]. It is similar to pollen of recent
62 *Holocheilus*, *Jungia*, and *Proustia*, being subprolate, tricolporate, microechinate and with a complex exine
63 structure [3].
- 64 5. **Stem age of Cichorieae excluding Scorzonerinae:** 22.0–125 Ma. The lower bound is based on the earliest
65 confirmed fossil pollen of Cichorieae, *Cichorium intyubs*-type pollen from the Molasse of the Paratethys,
66 which is at least 22 Ma old [28]. The pollen has three poral lacunae, six abporal lacunae (three at each side of
67 the equator), and six paraporal lacunae (three on each side of the equatorial ridge) [7], a trait combination
68 widely distributed in all subtribes except Scorzonerinae [60].
- 69 6. **Stem age of Sonchus + Launaea:** 5.4–125 Ma. The lower bound is based on *Sonchus oleraceus*-type pollen
70 from the Late Miocene, which resembles that of extant *Aetheorhiza*, *Hyoseris*, *Launaea*, and *Sonchus* [8]. Our
71 sampling included only the latter two genera.

72 The constraints for the *Ligularia-Cremanthodium-Parasenecio* complex and *Saussurea* below are based on 95% HPD
73 intervals inferred from this backbone.

74 **Ingroup: *Ligularia-Cremanthodium-Parasenecio* complex; outgroup scope: Tussilagininae**

- 75 1. **Root age:** 9.5–29.8 Ma.
- 76 2. **Crown age of *Ligularia*:** 2.32–16.85 Ma.
- 77 3. **Crown age of *Petasites* + *Tussilago*:** 1.09–15.18 Ma.

78 **Ingroup: *Saussurea*; outgroup scope: Cardueae**

- 79 1. **Crown age of *Saussurea*:** 2.27–13.98 Ma.

80 **Ingroup: *Lilium*, including *Nomocharis*; outgroup scope: Lilieae (Liliaceae)**

- 81 1. **Root (crown age of Lilieae):** 9.1–23.2 Ma. This is the 95% HPD interval for the node age estimated by Gao
82 *et al.* [23]. It is a secondary calibration for dating nodes with *Lilium*, derived from a fossil-based calibration of
83 Liliaceae and Smilacaceae.

84 **Ingroup: Meconopsis; outgroup scope: Papaveraceae**

85 1. **Crown age of Meconopsis:** 12–34 Ma. The bounds are based on the 95% HPD interval for the node age
86 estimated by Xiao [69], which used fossil calibrations from other taxa in Ranunculales.

87 **Ingroup: Microsoroideae; outgroup scope: Polypodiaceae**

- 88 1. **Root (crown age of Polypodiaceae):** 33.9–77 Ma. The lower bound is based on the earliest uncontroversial
89 fossil of Polypodiaceae, *Protodrynaria takhtajanii* from the Eocene of Siberia [61]. The maximum bound is
90 based on a secondary calibration, the upper bound of the 95% HPD for the crown age of polygrammoids [56].
- 91 2. **Crown age of Drynaria:** 5.3–66 Ma. The lower bound is based on a fossil of the extant species *D. propinqua*
92 from the late Miocene of SW China [65]. The upper bound is based on the assumption that the genus is
93 unlikely to have originated before the Cenozoic.
- 94 3. **Stem age of Polypodium:** 25.6–66 Ma. The lower bound is based on the earliest fossil record of the genus
95 from the early Oligocene of Czech Republic [33]. The upper bound is based on the assumption that the genus is
96 unlikely to have originated before the Cenozoic.
- 97 4. **Stem age of Pleopeltis:** 15.8–66 Ma. The lower bound is based on the oldest reliable fossil of the genus, from
98 the Miocene of the Dominican Republic [55]. The upper bound is based on the assumption that the genus is
99 unlikely to have originated before the Cenozoic.

100 **Ingroup: Pinaceae**

- 101 1. **Root (crown age of Pinaceae):** 152–200 Ma. The lower bound is based on the earliest fossil cone assigned to
102 Pinaceae, *Eathisstrobus* [54]. The upper bound is based on the absence of Pinaceae fossils before the Jurassic.
- 103 2. **Stem age of Larix:** 41–60 Ma. The bounds follow Leslie *et al.* [37]. The lower bound is based on the earliest
104 reliable fossil of *Larix*, *L. altoborealis* from the middle Eocene of Canada [36].
- 105 3. **Stem age of Picea:** 133–153 Ma. The bounds follow Leslie *et al.* [37]. The lower bound is based on *Picea*
106 *burtonii*, the earliest reliable fossil of *Picea* from the Early Cretaceous Apple Bay locality in British Columbia
107 [31].
- 108 4. **Stem age of Tsuga:** 41–90 Ma. The bounds follow Leslie *et al.* [37]. The lower bound is based on *Tsuga*
109 *swedaea* from the middle Eocene Buchanan Lake formation, Axel Heiberg Island [35].

- 110 **Ingroup: Polygonaceae; outgroup scope: Polygonaceae+Plumbaginaceae**
- 111 1. **Stem age of Polygonaceae:** 65.5–125 Ma. The lower bound is based on the fossil fruit *Polygonocarpum*
112 *johsonii* from the Maastrichtian of North Dakota, which exhibits wing venation patterns known only in
113 Polygonaceae [45].
- 114 2. **Stem age of *Polygonum*:** 28.1–125 Ma. The lower bound is based on the earliest fossil record of *Polygonum*
115 from the early Oligocene of western Siberia [19].
- 116 3. **Stem age of *Persicaria*:** 55.8–125 Ma. The lower bound is based on several *Persicaria*-type pollen fossils
117 reported from the Paleocene of Europe [24, 32] and accepted by Muller [47].
- 118 4. **Stem age of *Rumex*:** 16–125 Ma. The lower bound is based on seed and fruit fossils of the genus from the
119 middle Miocene of Germany [43].
- 120 5. **Crown age of *Muehlenbeckia*:** 12.7–125 Ma. The lower bound is based on the 12.7 Ma fossil of the extant
121 species *M. australis* from New Zealand [51, 57].

- 122 **Ingroup: Primuloideae; outgroup scope: Primulaceae sensu lato**
- 123 The upper bound for all constraints is based on the earliest fossil flowers of the “primuloid clade” (Maesaceae,
124 Theophrastaceae, Primulaceae, Myrsinaceae) from the Late Cretaceous (Campanian-Maastrichtian) Mira locality of
125 Portugal [22].
- 126 1. **Root (crown age of Primulaceae):** 48.6–72 Ma. The lower bound is based on the earliest fossil record of
127 Primulaceae, from the early Eocene London Clay Formation and assigned to *Ardisia* [16]. Fossils of
128 Myrsinoideae have also been reported from the early Eocene United States [30].
- 129 2. **Stem age of Primuloideae (Primulaceae s.s.):** 28–72 Ma. The lower bound is based on the earliest fossils of
130 Primuloideae, from the early Oligocene of Siberia [48].
- 131 3. **Stem age of *Primula*:** 15.96–72 Ma. The lower bound is based on the earliest unequivocal fossil of *Primula*,
132 *P. riosiae* [62].
- 133 4. **Stem age of *Androsace*:** 5.3–72 Ma. The lower bound is based on the earliest fossil seed of *Androsace*, from
134 the Miocene of western Siberia [19].

- 135 **Ingroups: *Rodiola* and Saxifragaceae+Grossulariaceae; outgroup scope: Saxifragales**
- 136 The ingroups were analyzed separately using a common set of calibrations.

137 1. **Root (crown age of Saxifragales):** 90–125 Ma. The lower bound is based on the Turonian fossil *Divisestylus*,
138 which shows flowers and fruits with well-preserved morphological characters that indicate a clear affinity to
139 Iteaceae [27].

140 2. **Stem age of *Itea*:** 49–125 Ma. The lower bound is based on the earliest fossil pollen assigned to *Itea* [26].

141 3. **Stem of *Ribes*:** 42–125 Ma. The lower bound is based on the earliest uncontroversial fossil leaves assigned to
142 *Ribes axelrodii* from the Eocene Bull Run floras [25].

143 **Ingroup: *Rhododendron*; outgroup scope: Ericaceae**

144 1. **Root (crown age of Ericaceae):** 89.8–125 Ma. The lower bound is based on the earliest fossil record of
145 Ericaceae, *Paleoenkianthus sayrevillensis* [49]. We also used this age as the upper bound for the following
146 constraints within the family.

147 2. **Stem age of *Rhododendron*:** 56–89.8 Ma. The lower bound is the earliest fossil record of the genus,
148 *R. newburyanum* from the Paleocene of South England [15].

149 3. **Stem age of *Erica*:** 5.33–89.8 Ma. The lower bound is based on the earliest fossil record of the genus,
150 *E. palaeoarborea* from the late Miocene of Europe [10].

151 4. **Stem age of *Empetrum*:** 11.62–89.8 Ma. The lower bound is based on the earliest fossil record of the genus,
152 from the middle Miocene of Denmark [21].

153 5. **Stem age of *Kalmia*:** 15.97–89.8 Ma. The lower bound is based on the earliest fossil record of the genus,
154 *K. saxonica* from the early Miocene of Germany [10].

155 **Ingroup: *Rosa*; outgroup scope: Rosales**

156 1. **Root (age of split between Rosaceae and Rhamnaceae):** 70–125 Ma. The lower bound is based on the oldest
157 fossil flower of Rhamnaceae, *Coahuilathus belindae*, from the late Campanian of Mexico [11].

158 2. **Crown age of subfamily Spiraeoideae excluding *Lyonothamnus*, supertribe Kerriodae, and tribe
159 Neilioeae:** 49.4–125 Ma. The lower bound is based on the earliest fossil of Spiraeoideae, *Paleorosa* from the
160 middle Eocene of British Columbia [6].

161 3. **Crown age of Amygdaleae:** 49.4–125 Ma. The lower bound is based on a fossil of *Prunus* from the middle
162 Eocene [17].

163 4. **Crown age of tribe Kerriae:** 49.4–125 Ma. The lower bound is based on the earliest fossil record for the tribe,
164 assigned to the genus *Neviusia*, from the middle Eocene of British Columbia [18].

165 5. **Stem age of *Rosa*:** 34–125 Ma. The lower bound is based on the earliest fossil record of the genus, from the
166 late Eocene Florissant Formation [44].

167 **Geographic range data**

168 Regional presence-absence matrices for ingroup species (Datasets S2 and S3) were assembled from the following
169 sources:

- 170 1. Flora of China (http://www.efloras.org/flora_page.aspx?flora_id=2)
- 171 2. Flora of North America (<http://floranorthamerica.org>)
- 172 3. Flora of Pakistan (http://www.efloras.org/flora_page.aspx?flora_id=5)
- 173 4. EURO+MEDI PlantBase (<http://www.emplantbase.org>)
- 174 5. USDA (<http://plants.usda.gov>)
- 175 6. Annotated Checklist of the Flowering Plants of Nepal (http://www.efloras.org/flora_page.aspx?flora_id=110)
- 176 7. Global Biodiversity Information Facility (<http://www.gbif.org>)
- 177 8. Biodiversity of the Hengduan Mountains (<http://hengduan.huh.harvard.edu>)
- 178 9. A county-level occurrence data set for vascular plants of the Hengduan Mountains [68, 72]

179 **Additional analyses of biotic assembly**

180 We assessed the robustness of our results to 2 factors: (1) the treatment of the Himalayas and QTP as a single
181 biogeographic area, and (2) the inclusion of non-angiosperms (the conifer clade Pinaceae and the fern clade
182 Microsoroideae) in estimates of assembly dynamics.

- 183 1. We recoded the species range data, treating the Himalayas and QTP as separate areas (Figure 1; Dataset S3).
184 We scored 210 out of the 4,668 species (4.5%) as occurring in the QTP. We then generated new ancestral range
185 reconstructions, and estimated rates of dispersal and *in situ* diversification through time, as described in
186 Materials and Methods. The results, summarized in Figures S3–S5, are virtually identical to the original results
187 with respect to Hengduan assembly dynamics.
- 188 2. Using the original Himalayas-QTP coding, we estimated rates of dispersal and *in situ* diversification through
189 time using only the 17 clades of angiosperms and present them in Figures S6–S8. The results do not change.
190 The only appreciable difference is that the time scale of biogeographic events is shortened, as the earliest
191 biogeographic events, from about 180–100 Ma, are all in Pinaceae.

192 **BAMM analyses of diversification rate**

193 **Sampling fractions**

194 We assigned sampling fractions at the finest level of taxonomic resolution possible, estimated from the most recent
195 phylogenetic treatments available. This was generally at the level of genus, but in cases where genera were not
196 confidently resolved as monophyletic, we assigned sampling fractions at higher taxonomic levels (tribe and
197 subfamily). For analyses of single genera larger than 100 species, we attempted to estimate sampling fractions of
198 infrageneric taxa. This was possible at the level of section for *Rhododendron* [20] and *Acer* [70]. For the others,
199 however, infrageneric classifications were sufficiently incongruent with phylogeny as to require the use of global
200 sampling fractions. This was the case for *Allium* [38], *Lilium* [23], *Rosa* [9], *Saussurea* [63], and *Thalictrum* [59].

201 **Comparisons with previous studies**

202 Shifts in diversification rate were studied previously in 3 of our sampled clades. Here we comment briefly on
203 differences between those results and ours.

- 204 1. *Primulaceae*.—de Vos *et al.* [62] used a variety of methods, but not BAMM, to investigate rate heterogeneity in
205 a phylogeny of Primulaceae, focusing on the hypothesis that faster diversification is associated with
206 heterostyly. Two of those methods, MEDUSA [1] and SymmeTREE [13], are similar to BAMM in that they
207 infer the locations of rate shifts without *a priori* hypotheses; but they are otherwise very different in their model
208 assumptions and algorithmic details. Unfortunately, the phylogeny from de Vos *et al.* [62] is not available on
209 TreeBASE (despite what is stated in the paper) so we were unable to analyze it with BAMM for comparison.
210 One difference between MEDUSA and BAMM is in their default assumptions about time-variable
211 diversification: MEDUSA assumes time-constant regimes, while BAMM by default does not. We re-analyzed
212 our Primulaceae tree with this option turned on in BAMM. This supported one increase in diversification—in
213 the heterostylous clade, as found by de Vos *et al.* [62].
- 214 2. *Rhododendron*.—Schwery *et al.* [58] used BAMM to analyze a phylogeny of Ericaceae as a whole, in which
215 *Rhododendron* was represented by 61 species; in comparison, our sampling included 351 species. They found
216 support for one shift within *Rhododendron* (section *Ponticum*) that corresponds to one of the 3–5 shifts in our
217 analysis.
- 218 3. *Lilium*.—Our taxon sampling and sequence data were taken from Gao *et al.* [23]. In that study, the authors
219 used LASER [52] to estimate speciation and extinction rates for the phylogeny as a whole, and for selected
220 clades, with results that are somewhat inconclusive and difficult to compare with ours.

Table S1: Global and regional sampling of clades.

clade	global			Hengduan Mountains			Himalayas-QTP			temperate/boreal East Asia		
	total	sampled	%	total	sampled	%	total	sampled	%	total	sampled	%
<i>Acer</i>	129	118	91	45	29	64	24	15	63	80	72	90
<i>Allium</i>	800	378	47	34	29	85	55	37	67	89	100	89
Clematidinae+												
Anemoninae	495	177	36	76	32	42	45	26	58	152	72	47
Delphineae	756	312	41	225	74	33	83	44	53	90	51	57
<i>Cyananthus</i>	66	47	71	41	28	68	26	24	92	14	10	71
<i>Isodon</i>	100	63	63	55	40	73	20	9	45	36	24	67
<i>Ligularia-</i>												
<i>Cremanthodium-</i>												
<i>Parasenecio</i> complex	380	75	20	152	60	39	62	12	19	148	27	18
<i>Lilium</i> (incl.												
<i>Nomocharis</i>)	122	104	85	36	30	83	18	15	83	44	41	93
<i>Meconopsis</i>	54	47	87	25	22	88	36	34	94	2	2	100
Microsoroideae	248	147	59	45	42	93	38	35	92	80	66	83
Pinaceae	234	226	97	34	32	94	26	24	92	63	63	100
Polygoneae	663	257	39	92	61	66	85	75	88	160	127	79
Primulaceae	900	354	39	205	114	56	150	68	45	80	55	69
<i>Rhodiola</i>	70	57	81	32	28	88	37	30	81	34	20	59
<i>Rhododendron</i>	1000	351	35	237	120	51	124	42	34	300	105	35
<i>Rosa</i>	175	102	58	49	27	55	29	20	69	64	35	55
<i>Saussurea</i>	416	147	35	108	73	68	130	63	48	157	56	36
Saxifragaceae+												
Grossulariaceae	760	313	41	209	54	26	155	45	29	170	102	60
<i>Thalictrum</i>	150	104	69	38	34	89	40	25	63	48	32	67

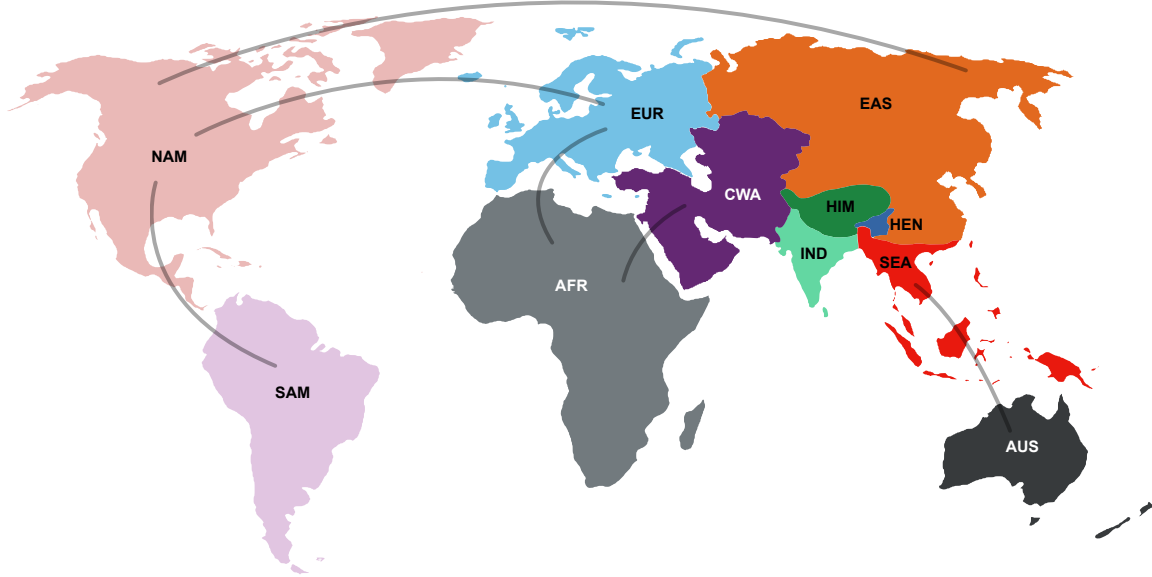
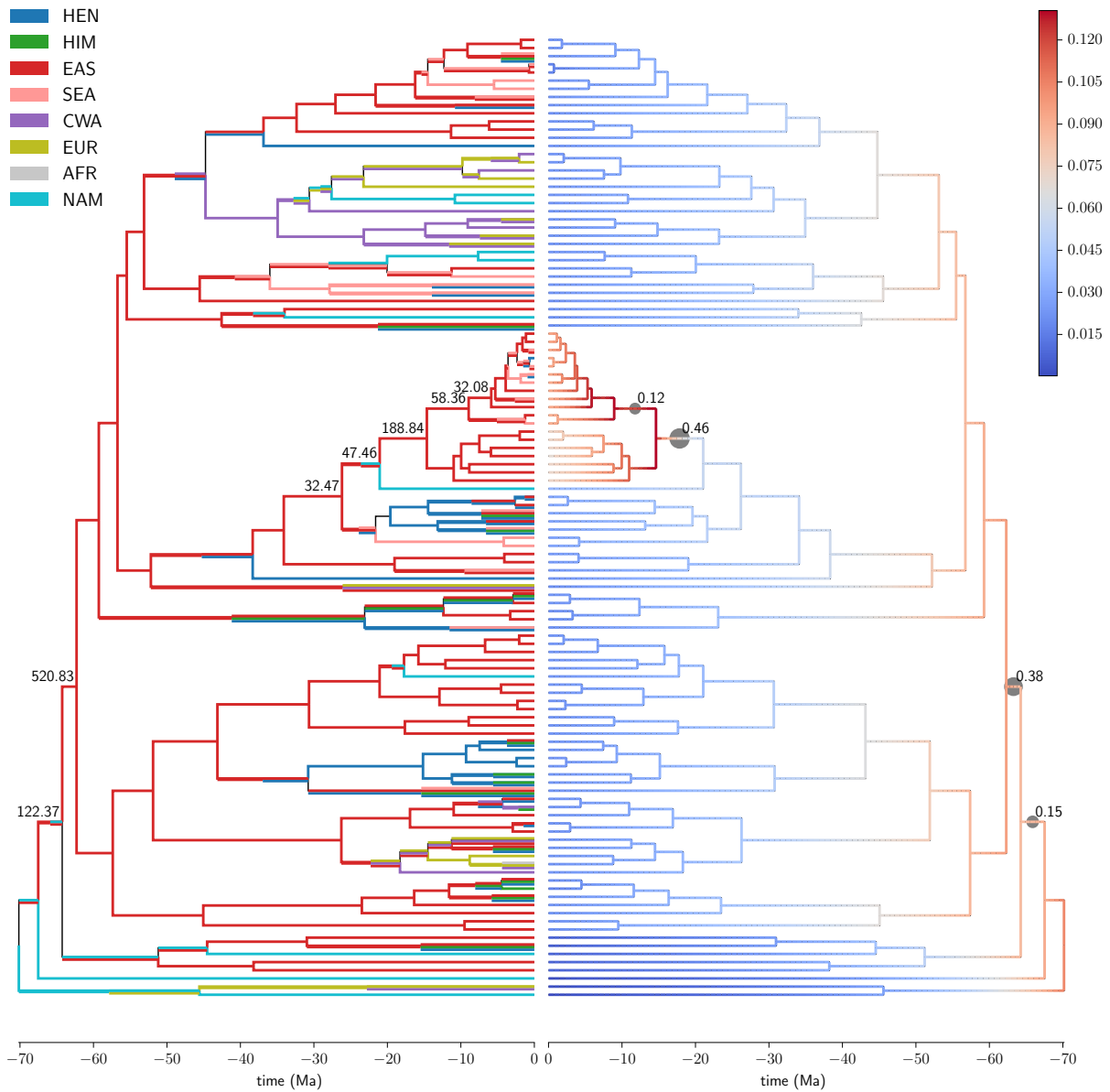
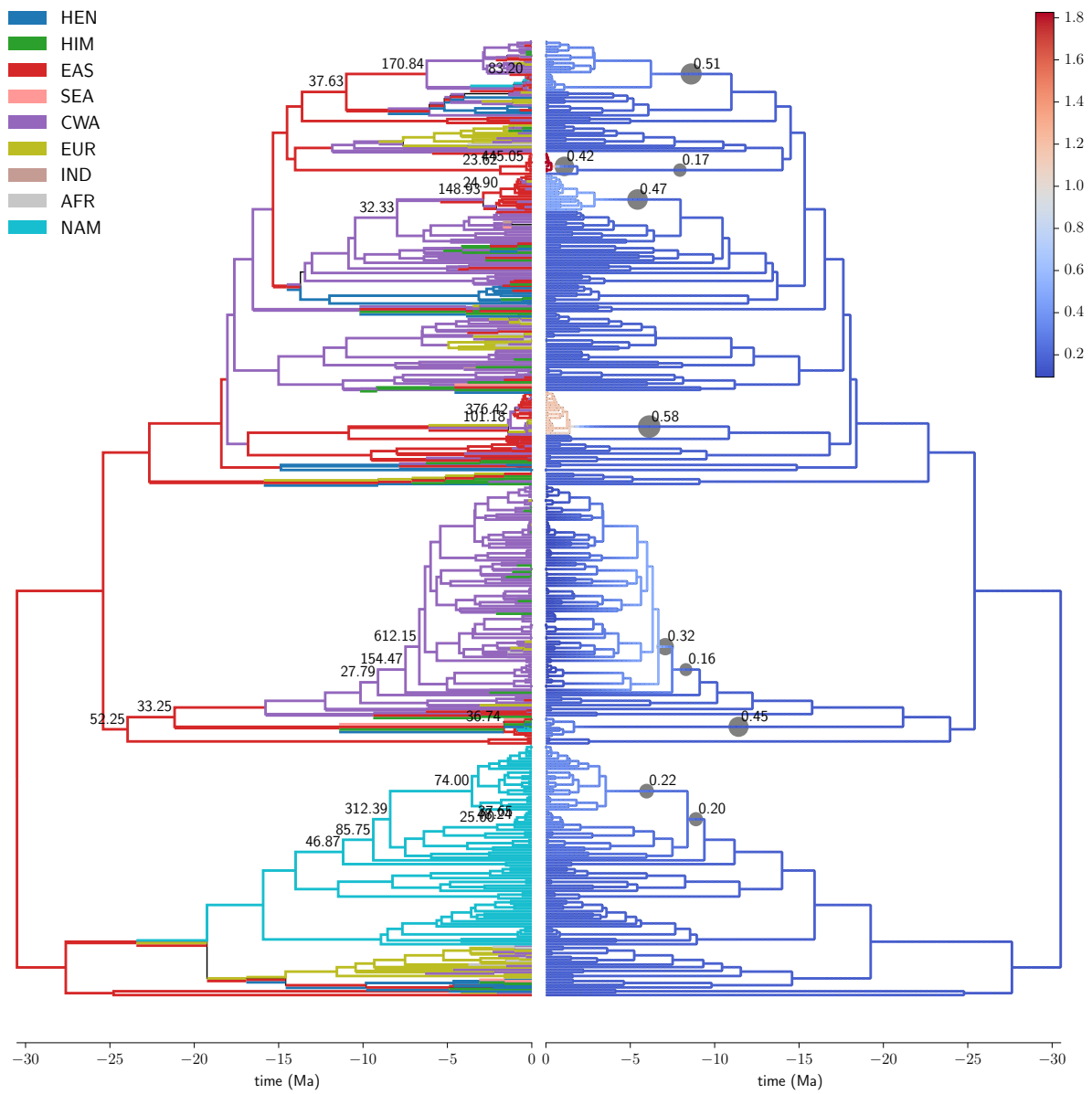
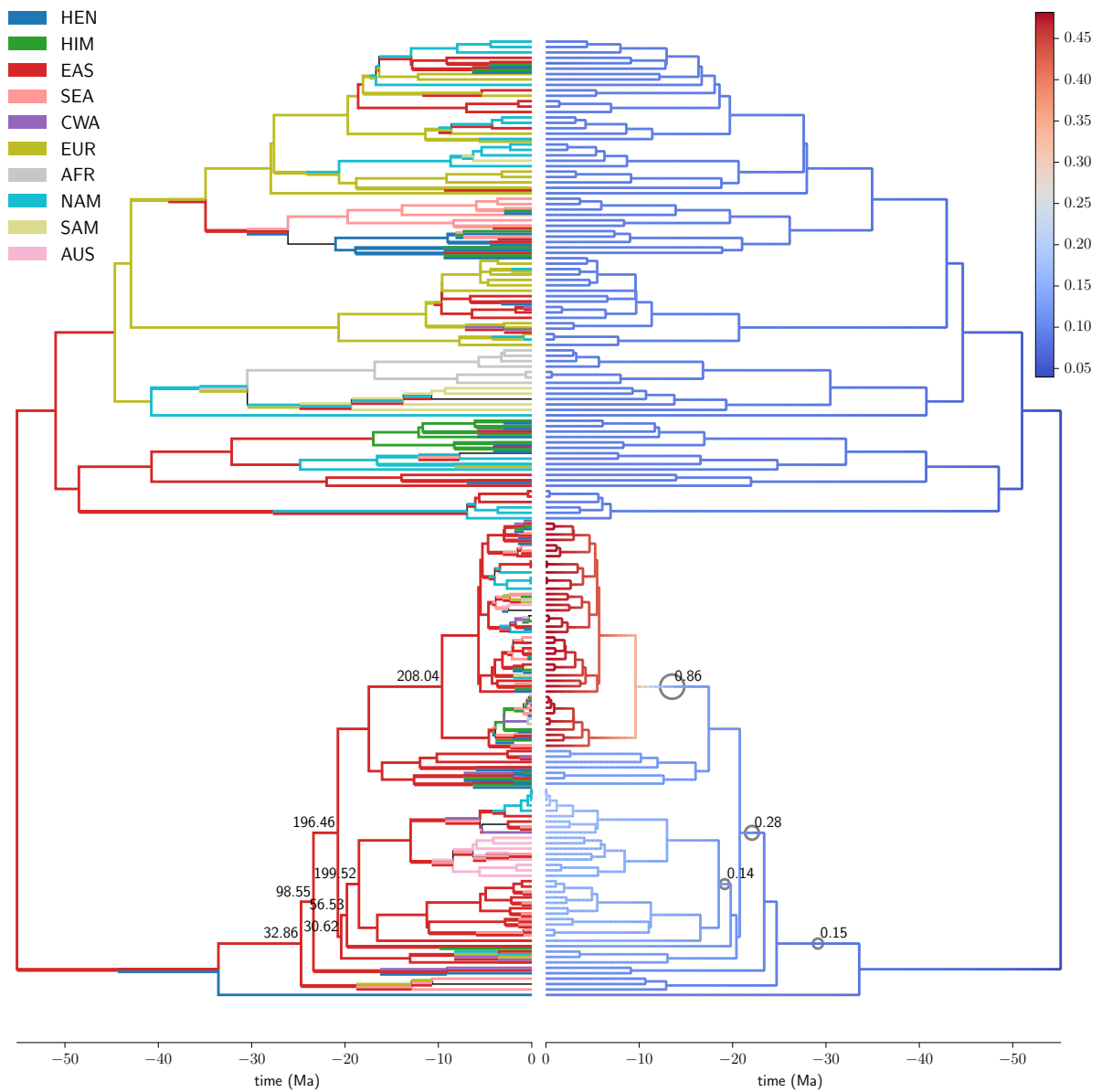


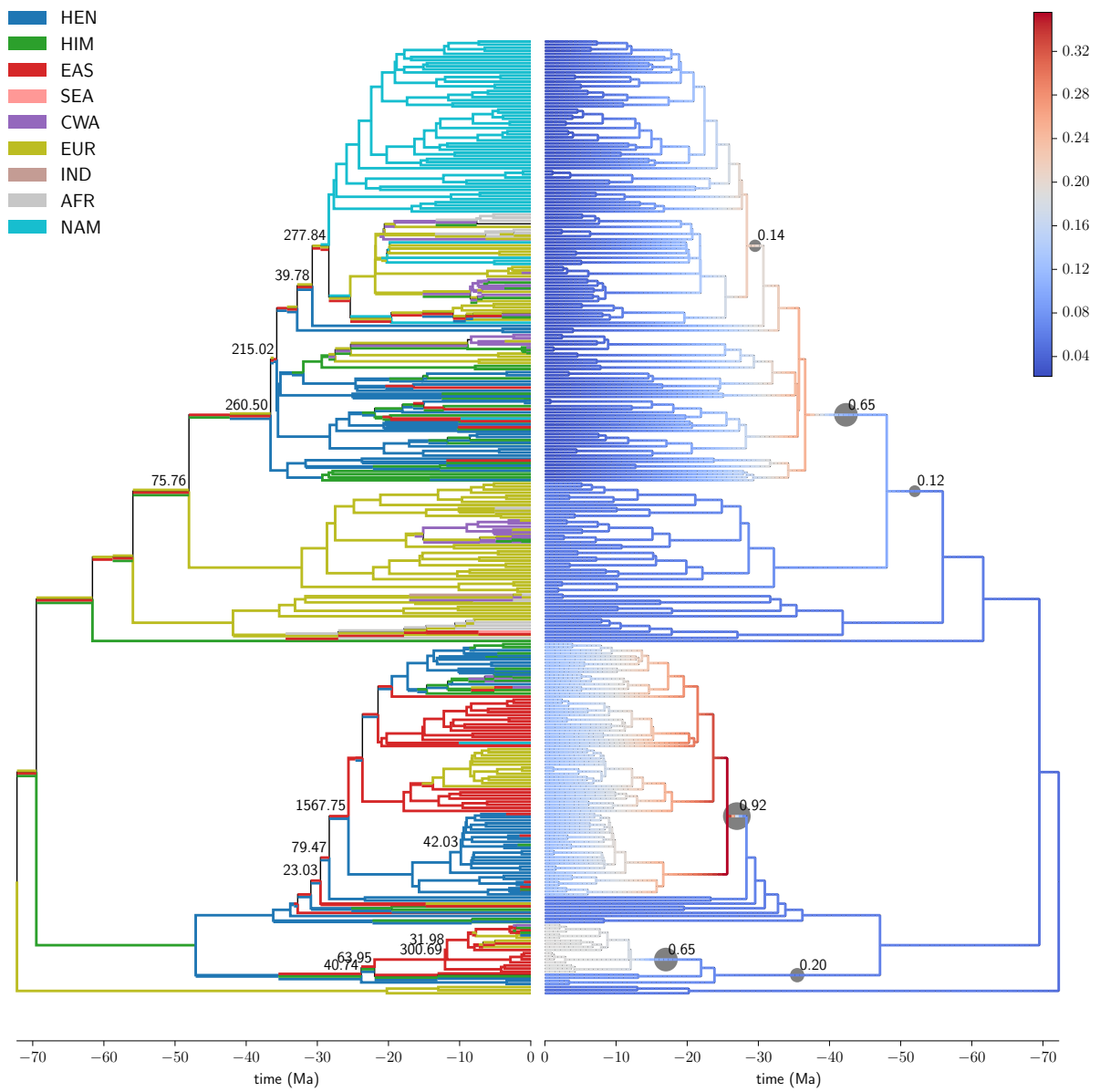
Figure S1: Map of the 11 geographic regions used for ancestral range analyses in Lagrange. HEN = Hengduan Mountains, HIM = Himalayas-QTP, EAS = temperate/boreal East Asia, SEA = Southeast Asia, CWA = Central/Western Asia, EUR = Europe, IND = India, AFR = Africa, NAM = North America, SAM = South America, AUS = Australasia. Lines and common borders indicate dispersal routes allowed in Lagrange.

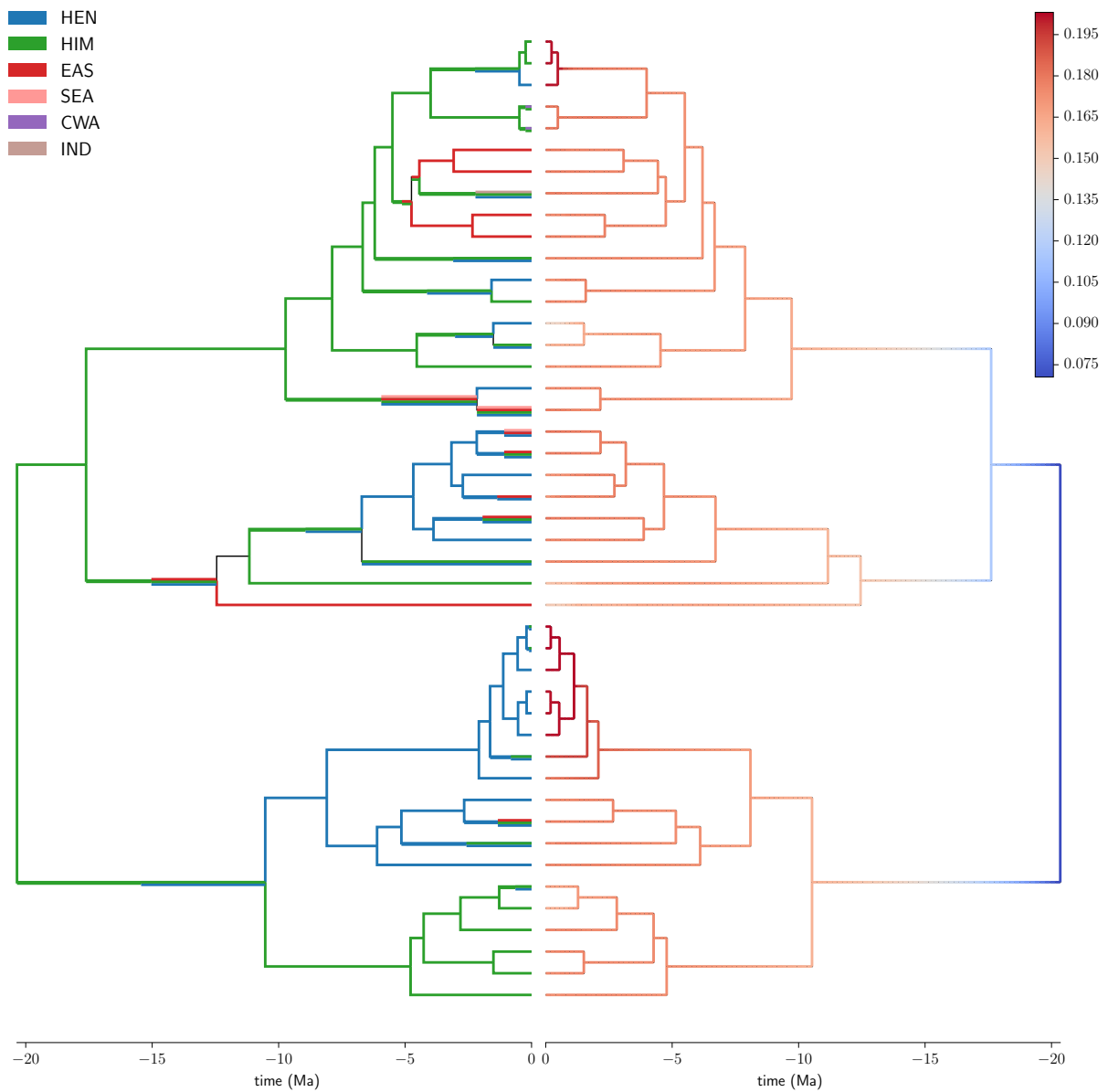
Figure S2: Reconstructions of ancestral geographic range (left) and net diversification rate (right) on the maximum clade credibility tree, with branch lengths set to posterior means, for each ingroup taxon (excluding *Rhododendron*, shown as Fig. 5). Ancestral ranges are maximum-likelihood estimates at the start and end of each branch. Net diversification values are branch-segment means of the posterior distribution estimated by BAMM. Filled circles on the right indicate branches that appear in the 95% credible set of distinct shift configurations, with the size and label of a circle indicating the cumulative probability of the branch over all configurations in the credible set. On the left, the marginal odds ratio for a shift in diversification regime along a branch is drawn for branches where the ratio exceeds 20. Geographic regions are coded as follows: HEN, Hengduan Mountains; HIM, Himalayas-QTP; EAS, temperate-boreal East Asia; SEA, Southeast Asia; CWA, central/western Asia; EUR, Europe; IND, India; AFR, Africa; NAM, North America; SAM, South America; AUS, Australasia.

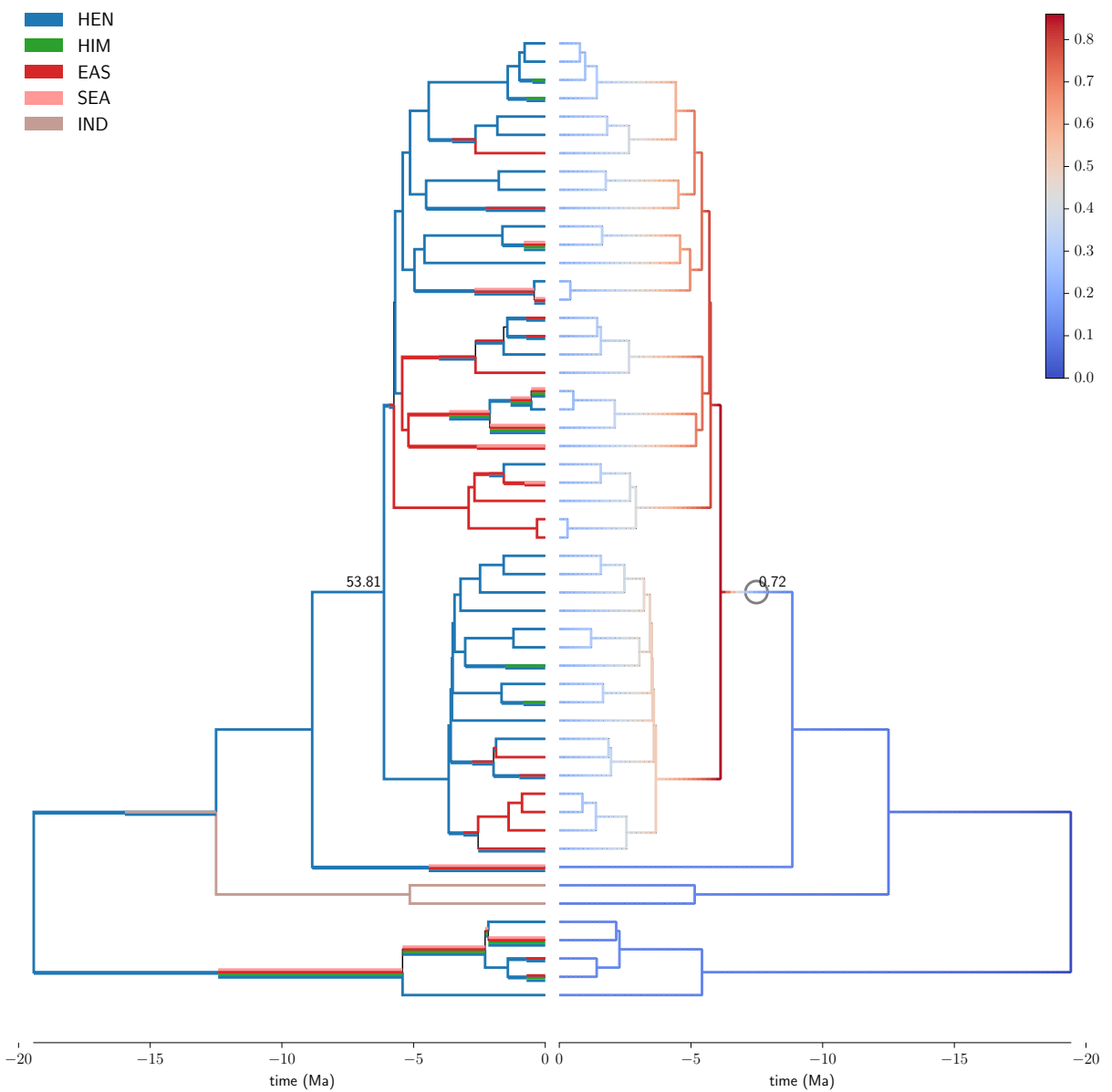


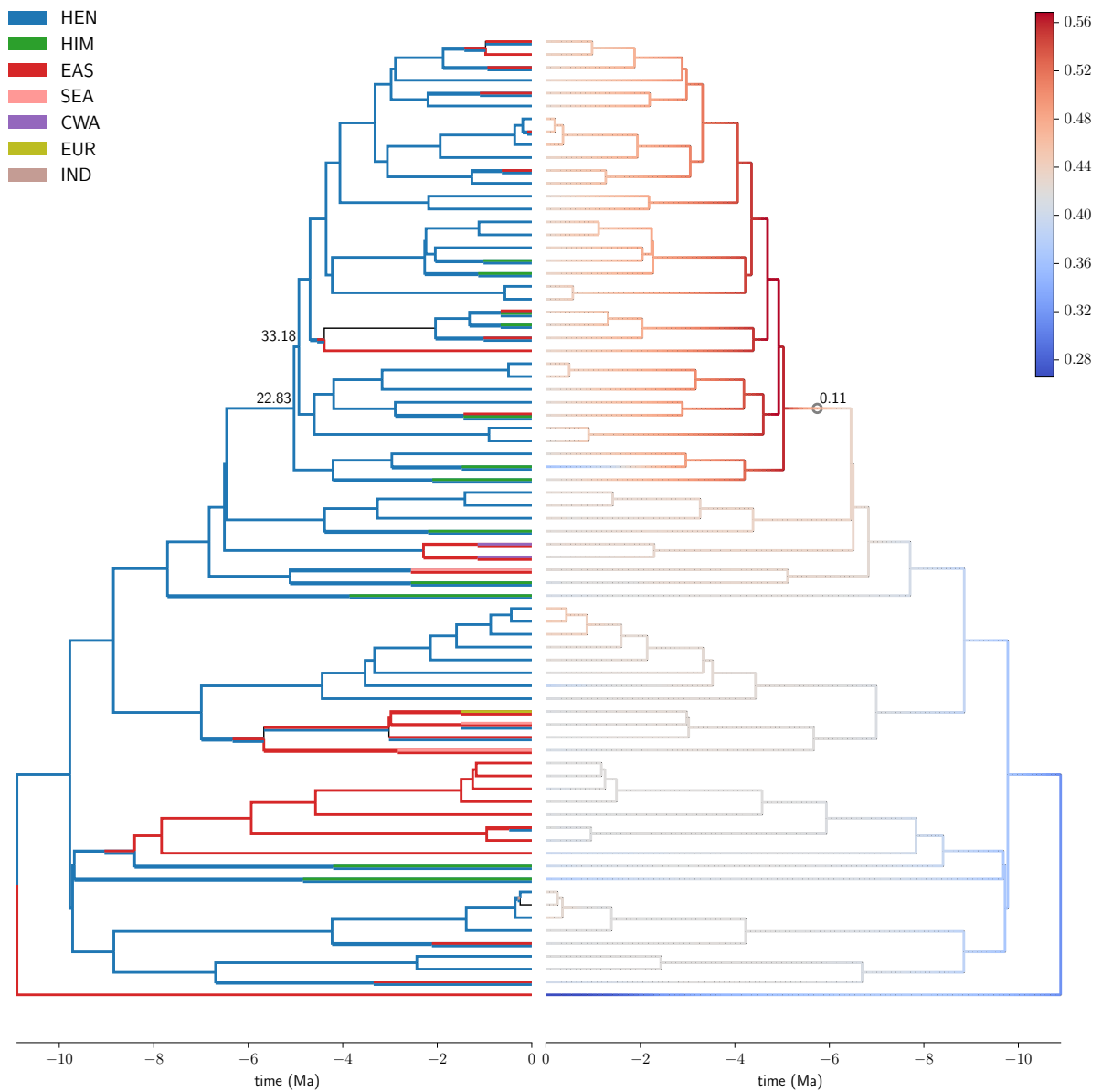


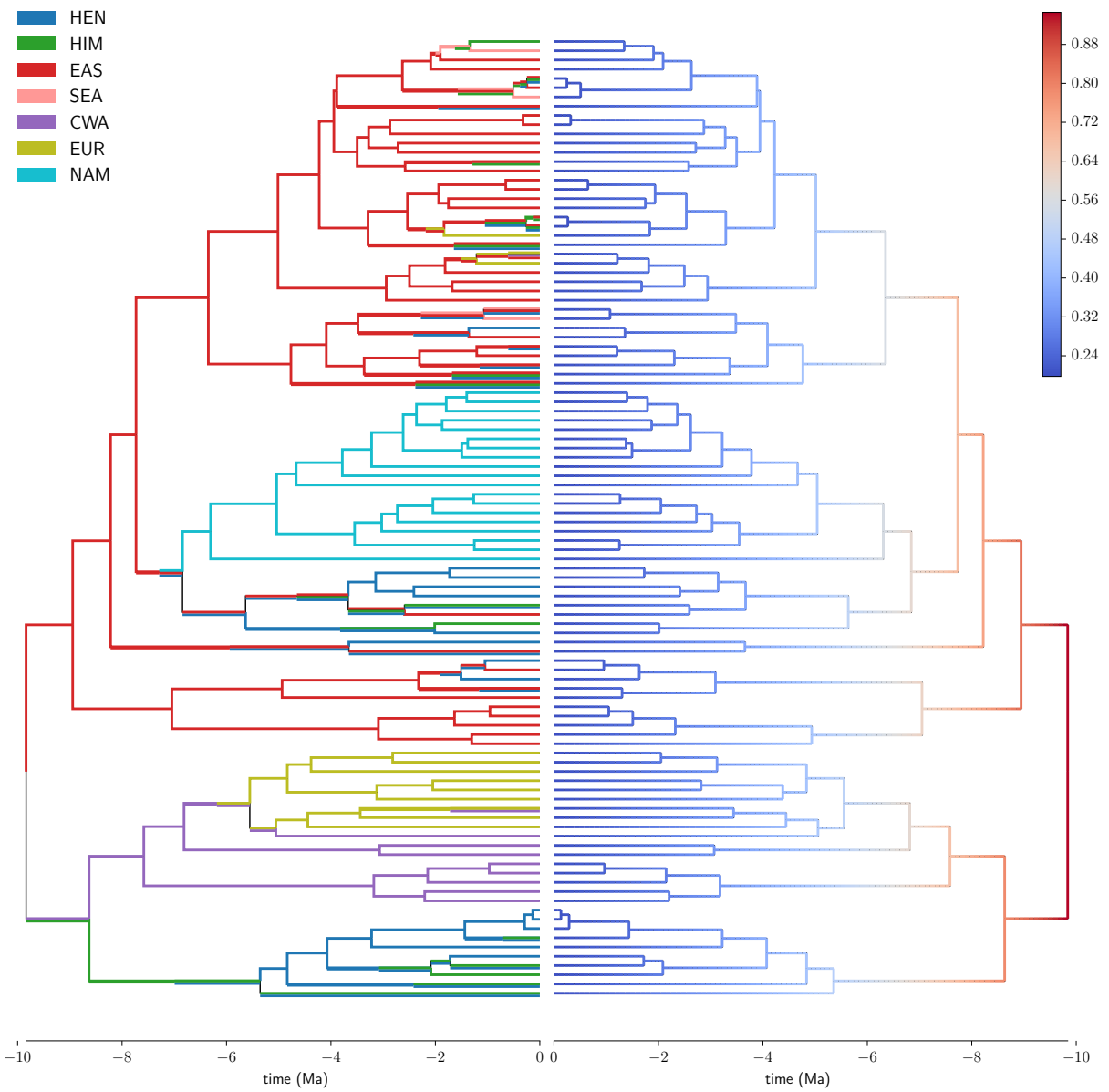


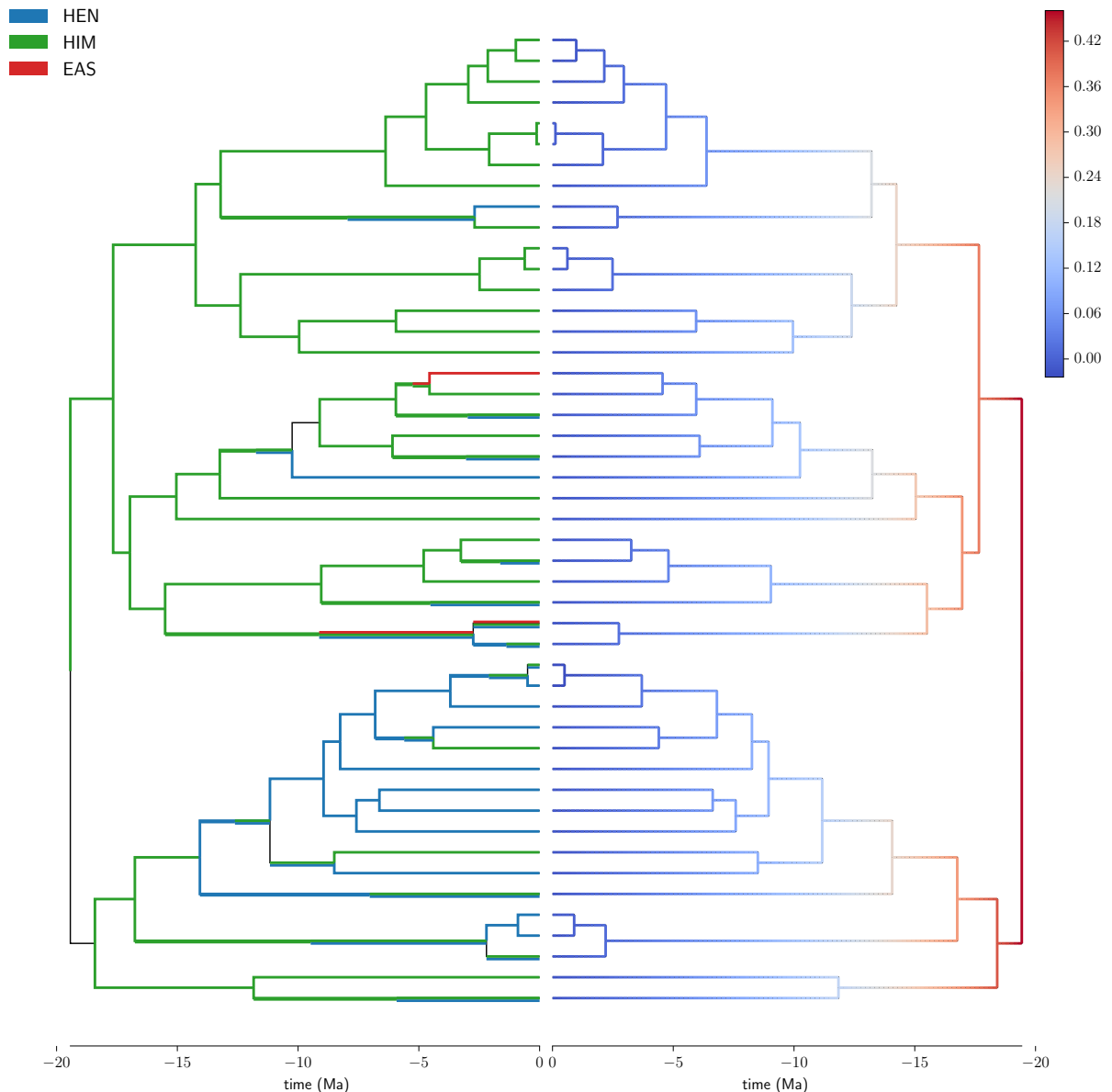


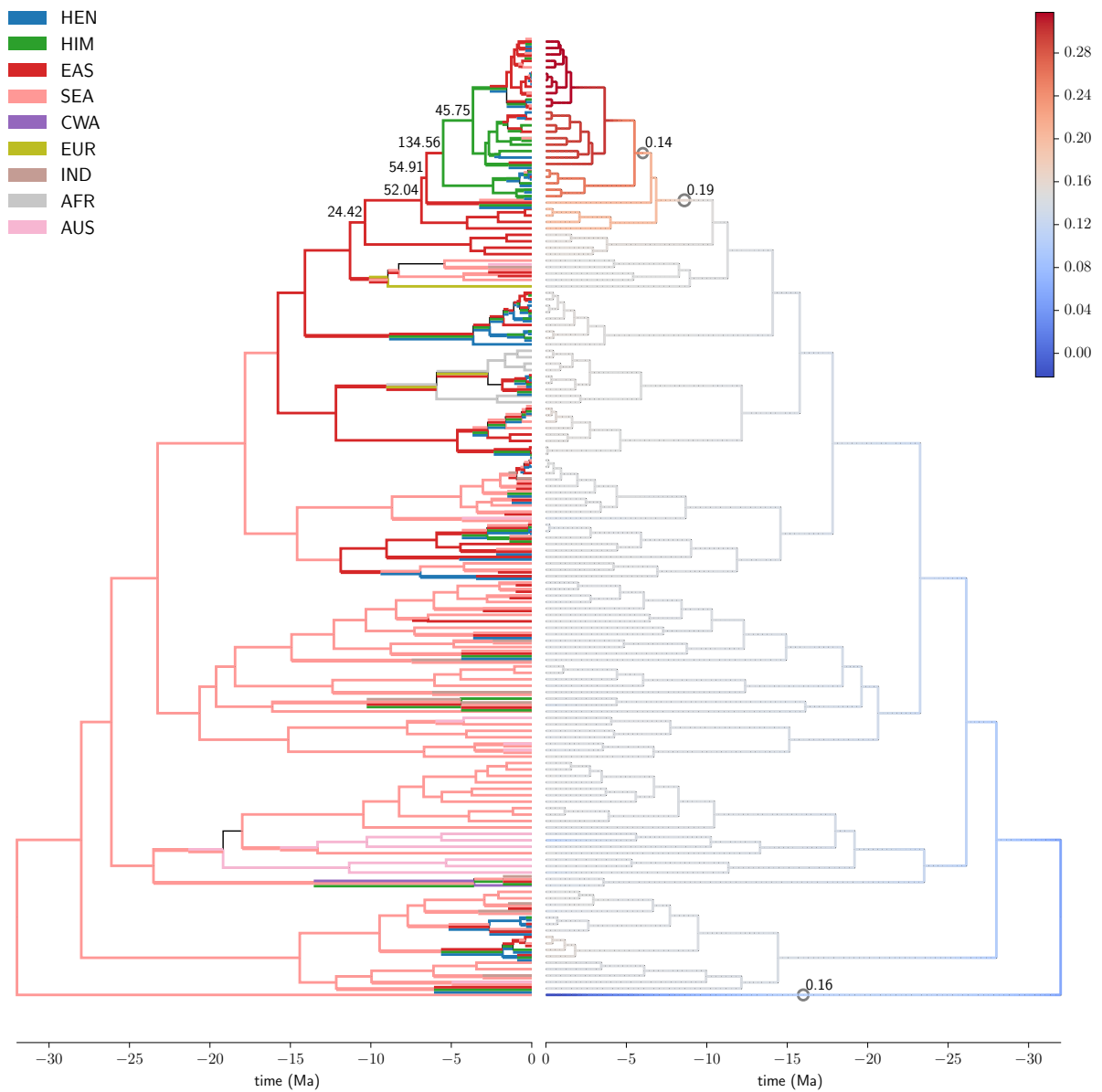




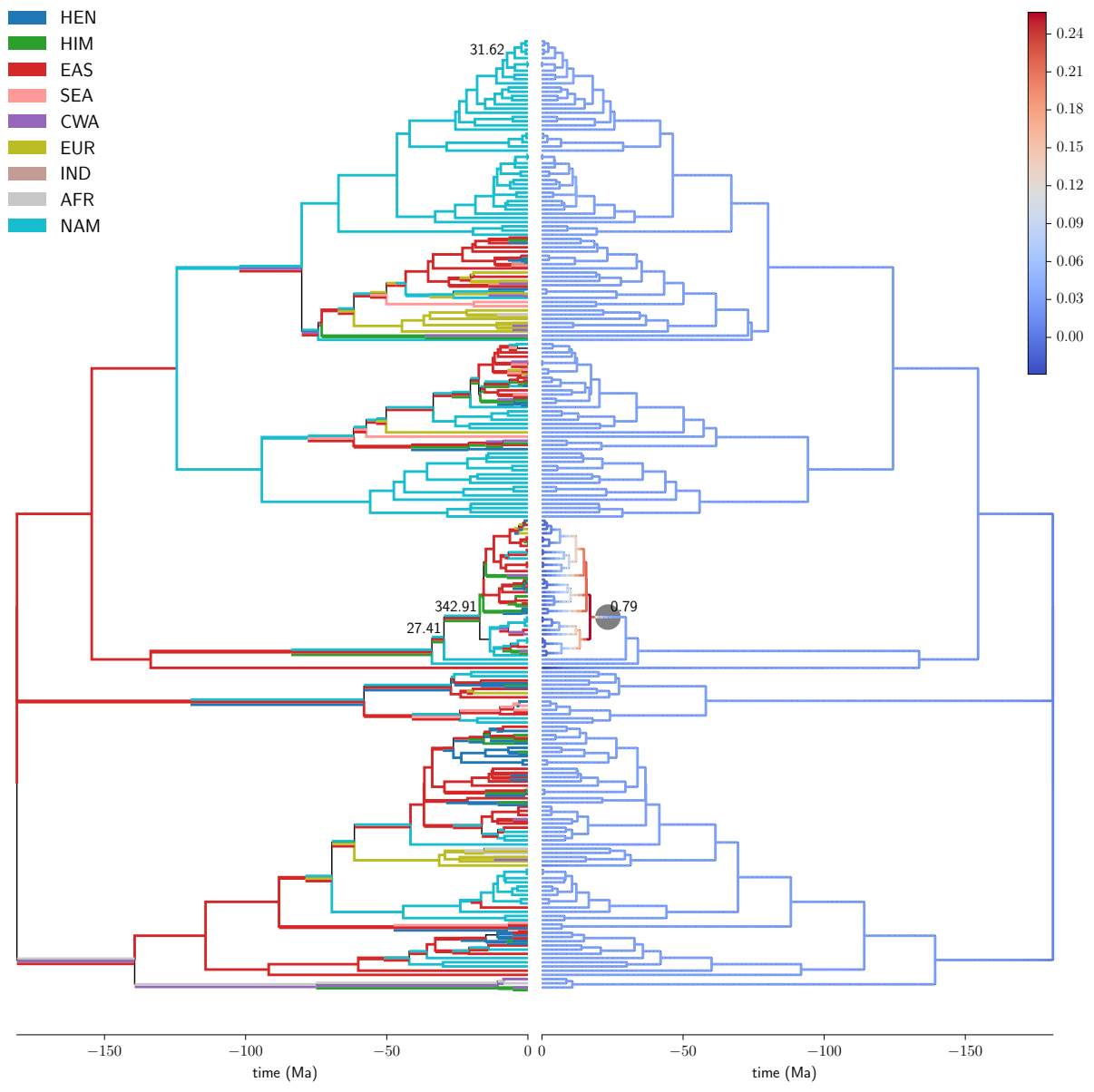


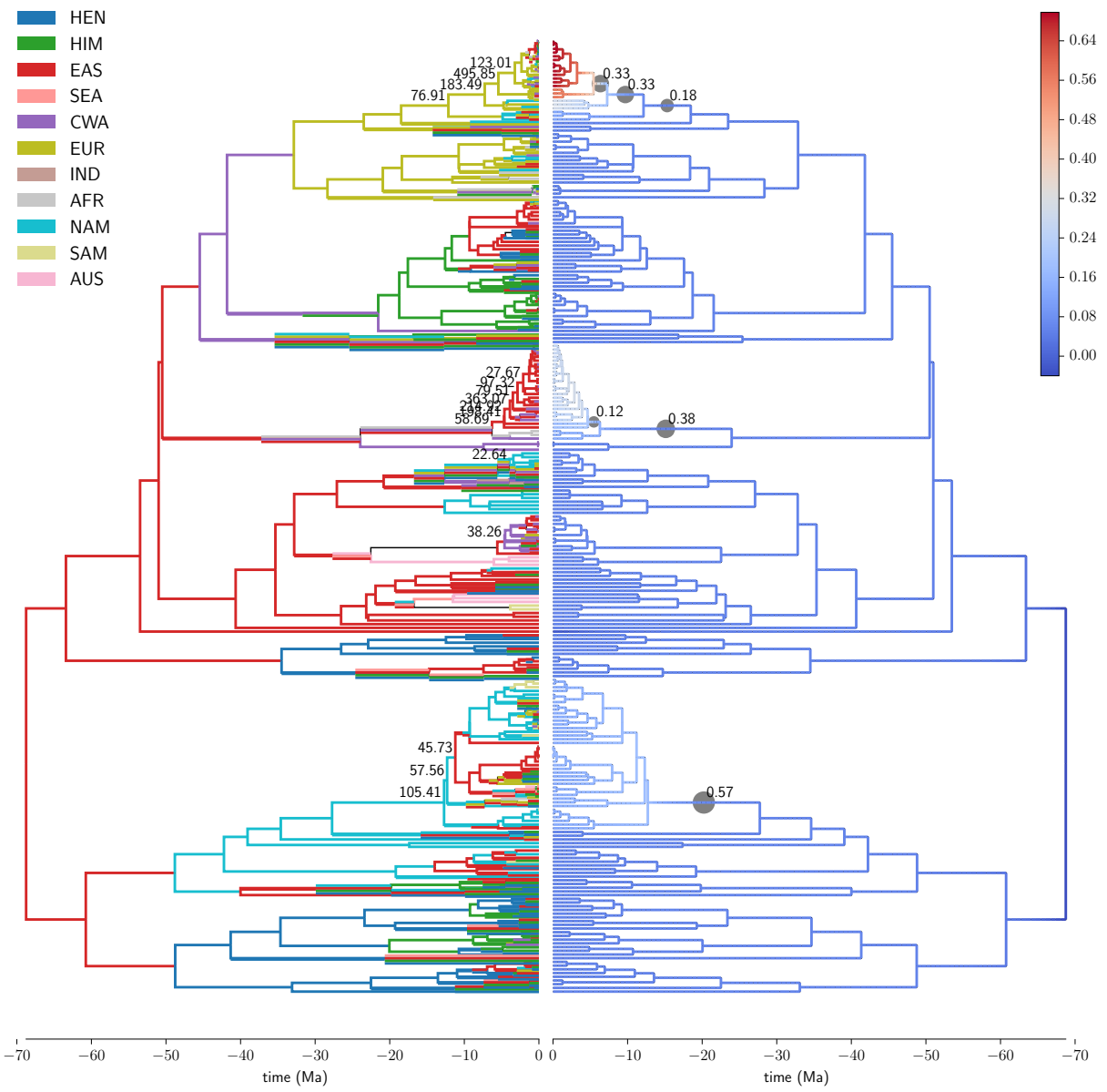


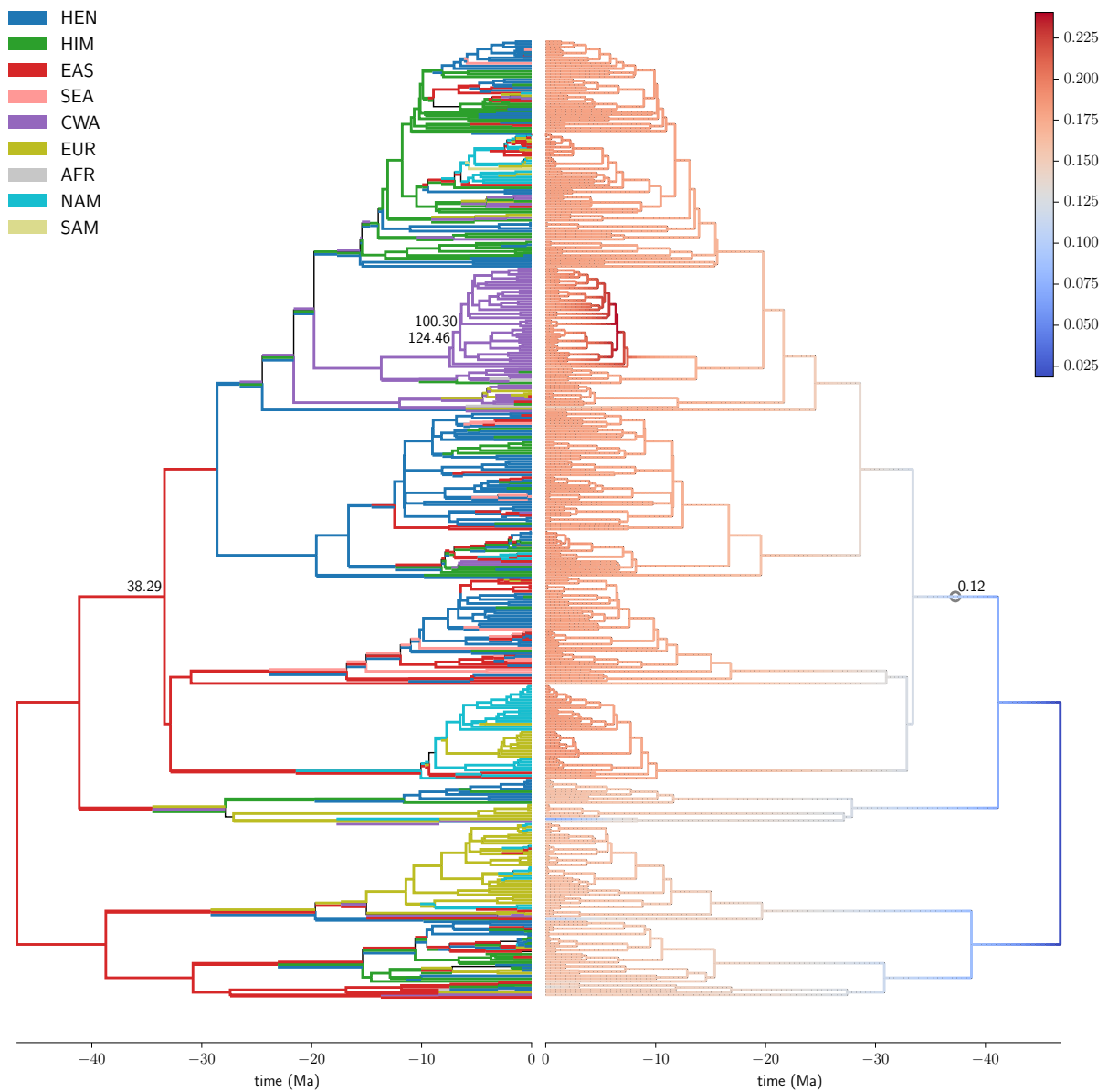


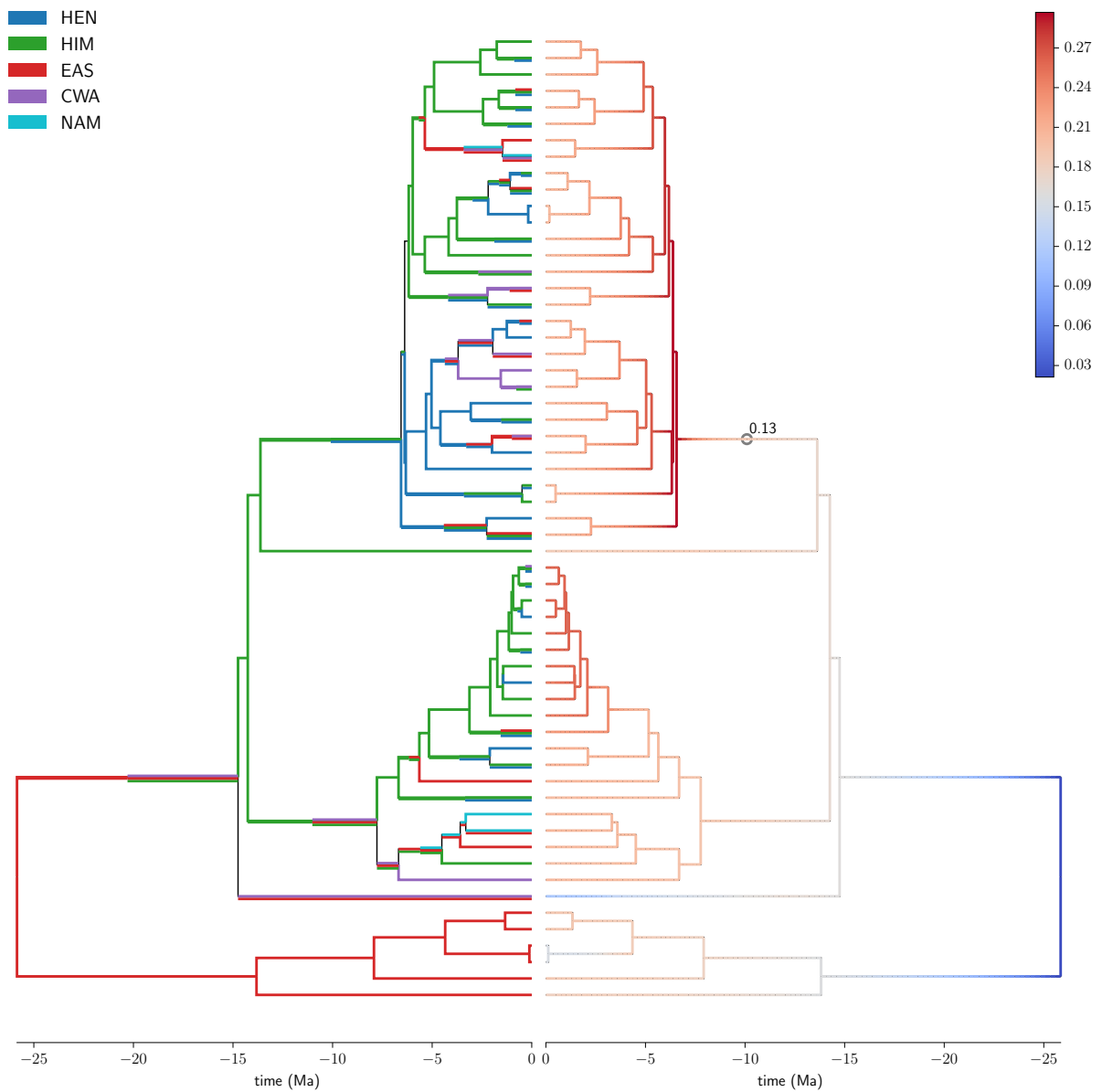


S2J Microsoroideae

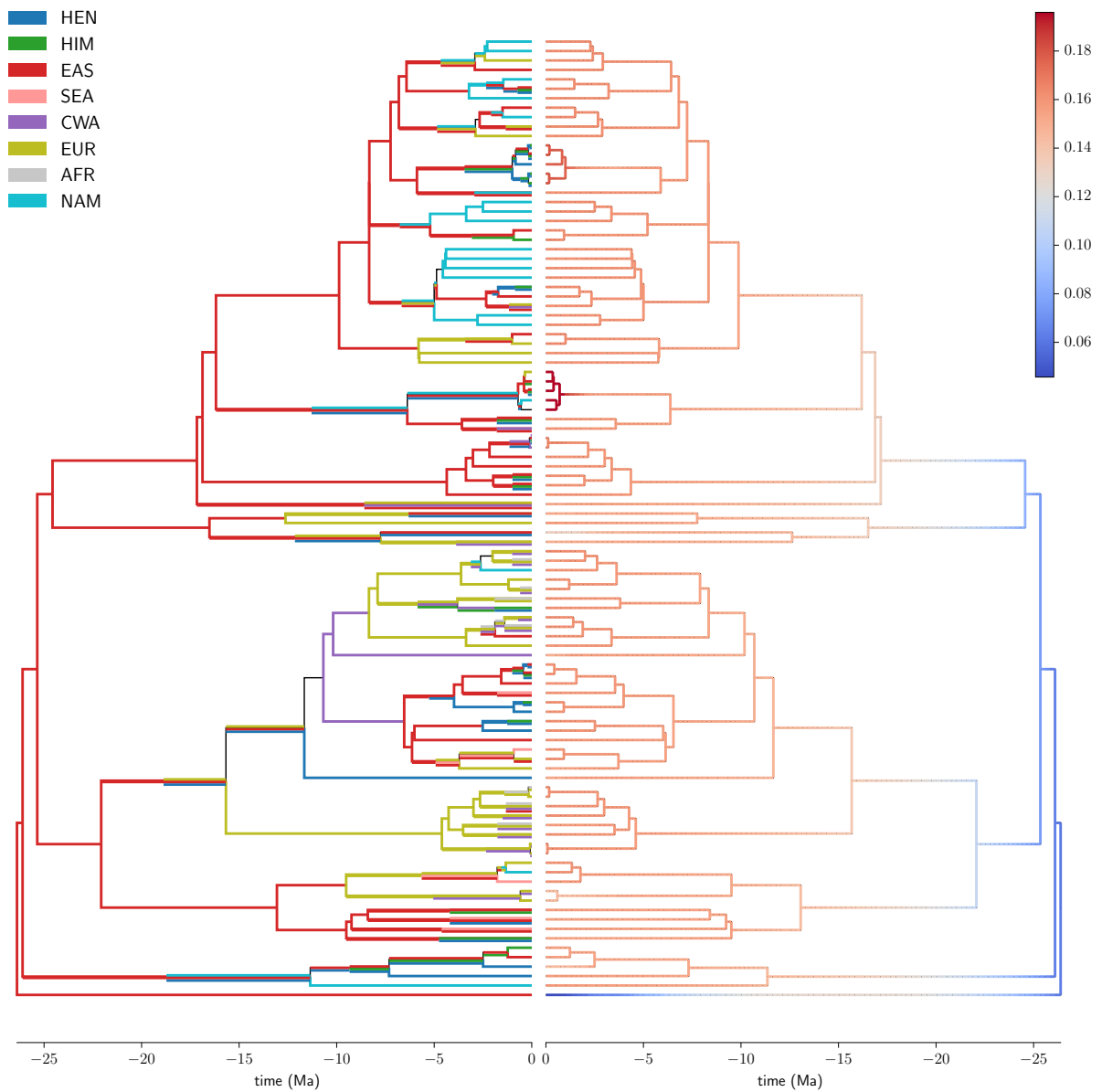


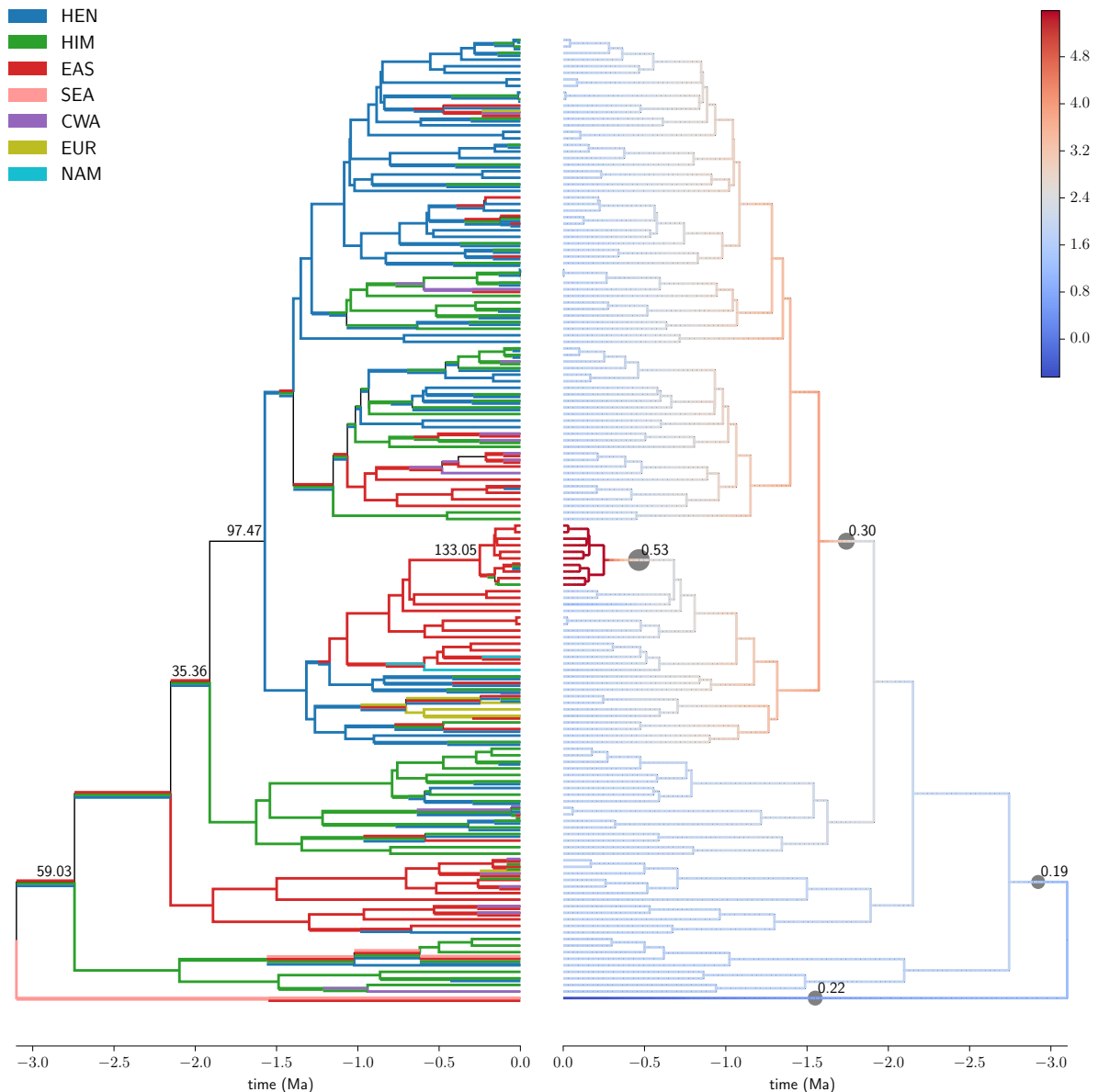


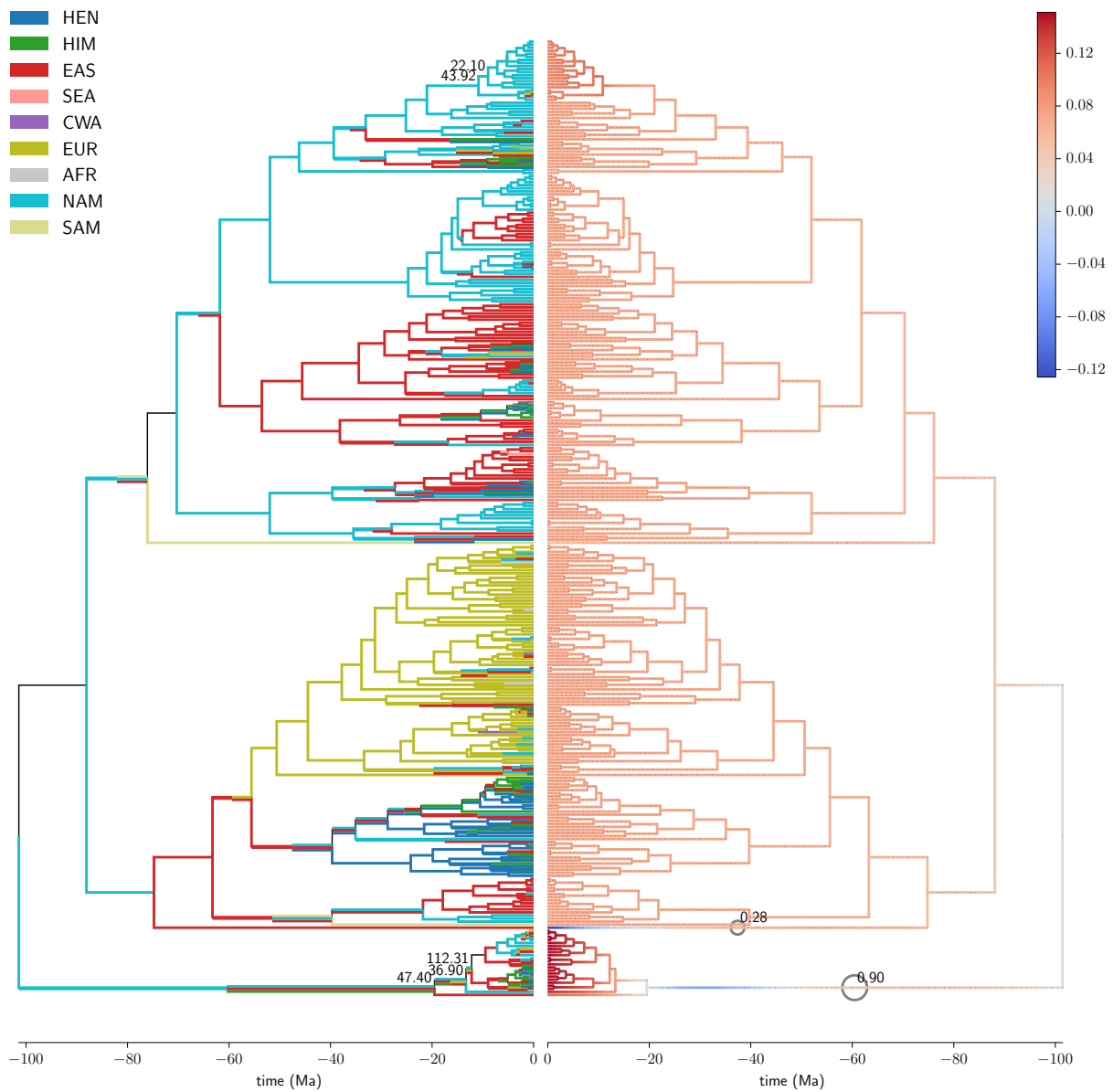


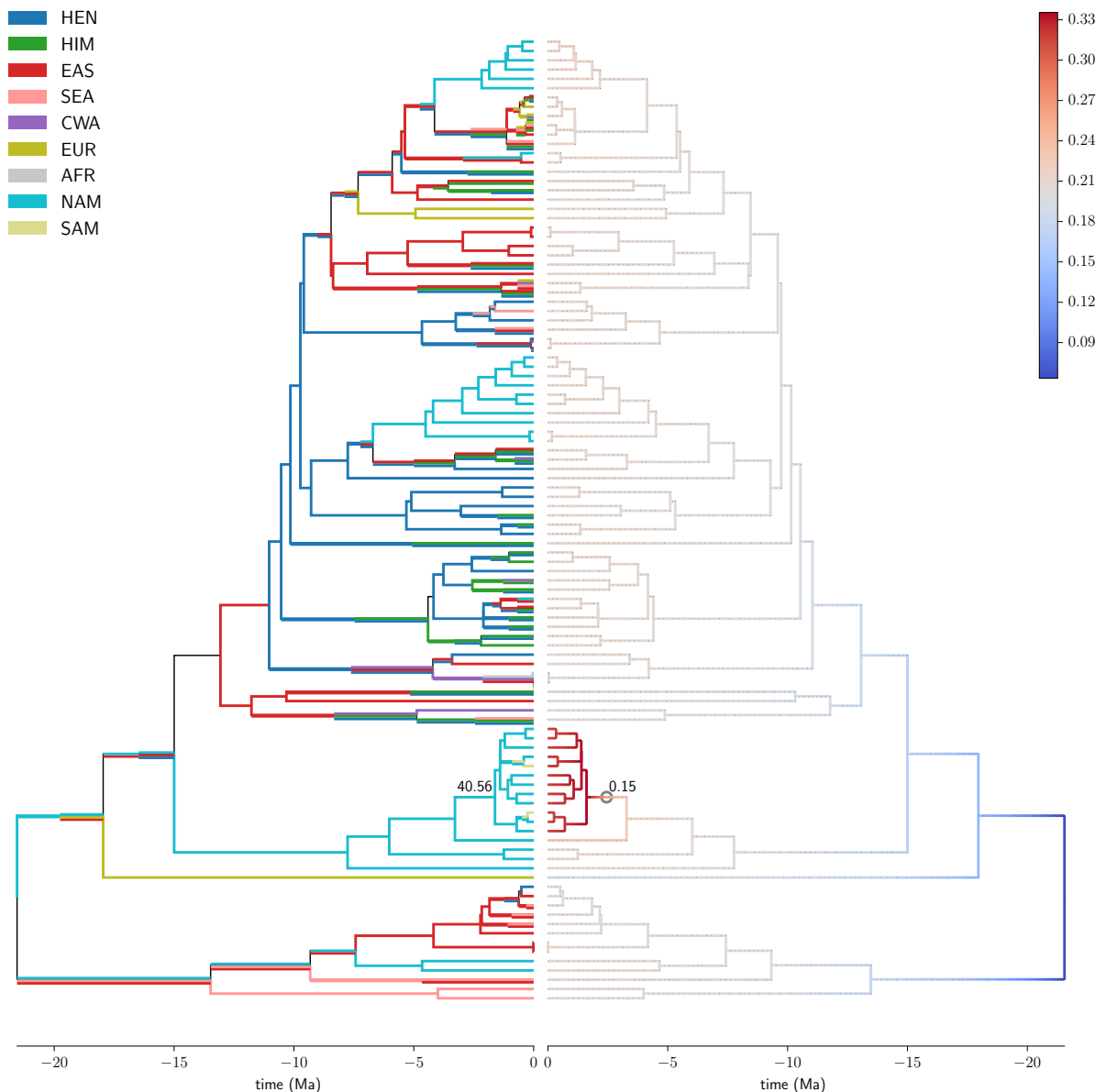


S2N *Rhodiola*









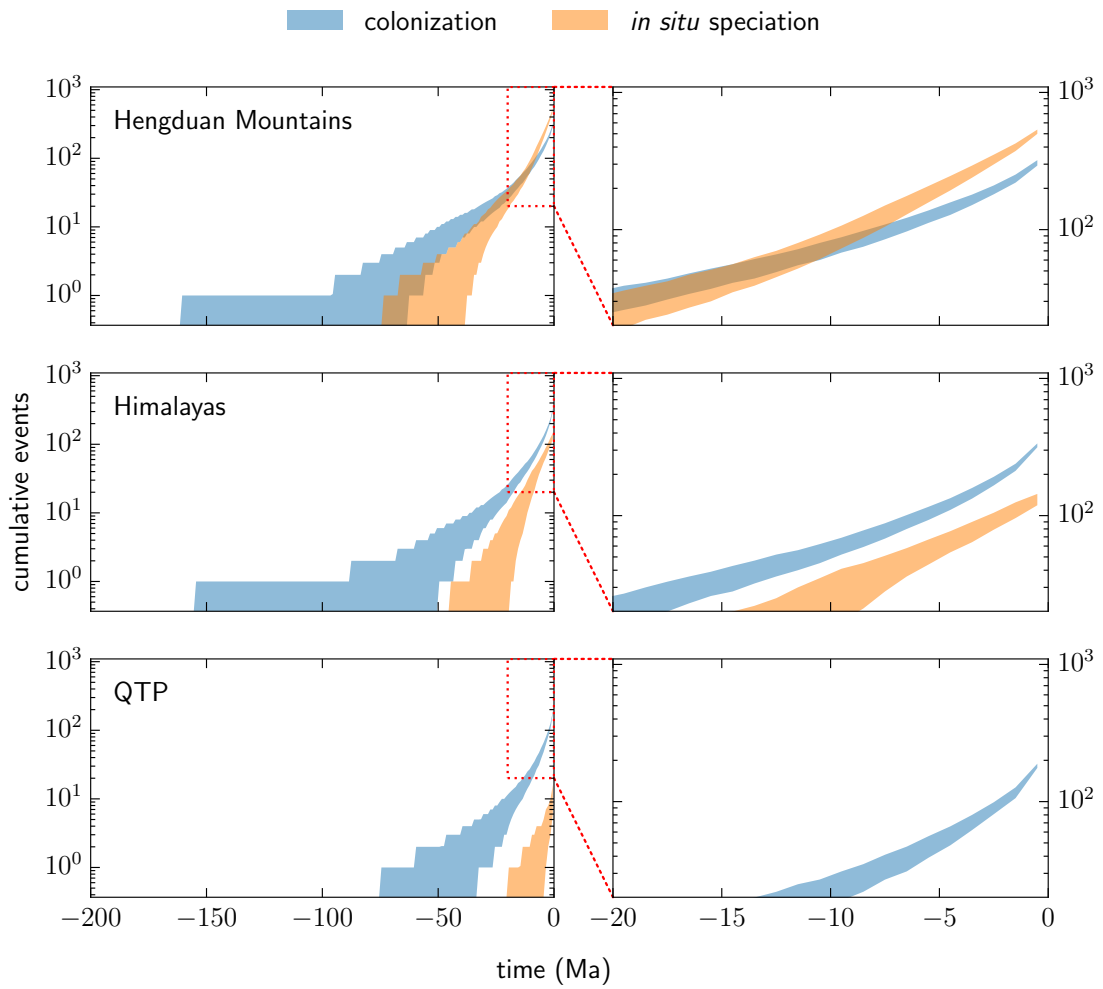


Figure S3: Cumulative numbers of colonization and *in situ* speciation events in 19 plant clades through time, as described in Figure 2. Here, the same analysis is shown, except that is based on ancestral range reconstructions in which the Himalayas and QTP were coded as distinct areas. The dynamics of the Hengduan region are essentially unchanged from the original analysis.

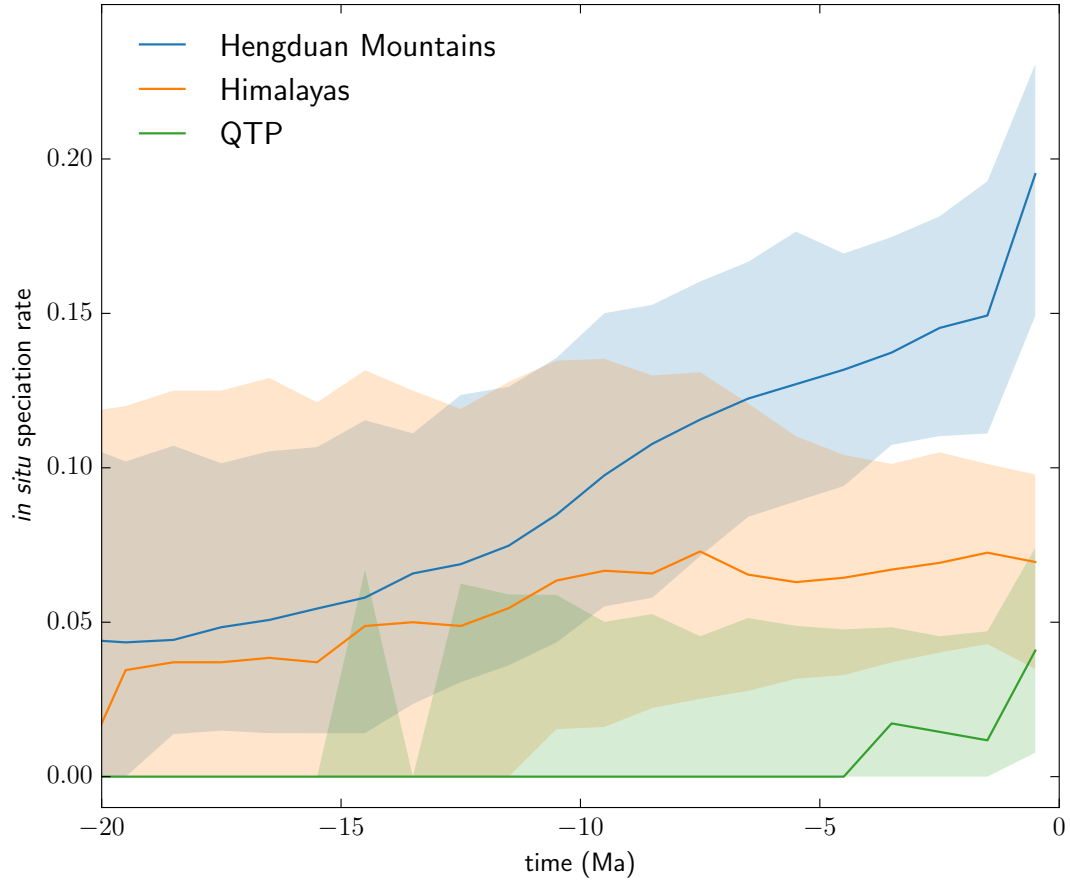


Figure S4: Rolling estimates of *in situ* speciation rates through time, as described in Figure 3, showing the results from treating the Himalayas and QTP as distinct areas. The dynamics of the Hengduan region are essentially unchanged from the original analysis.

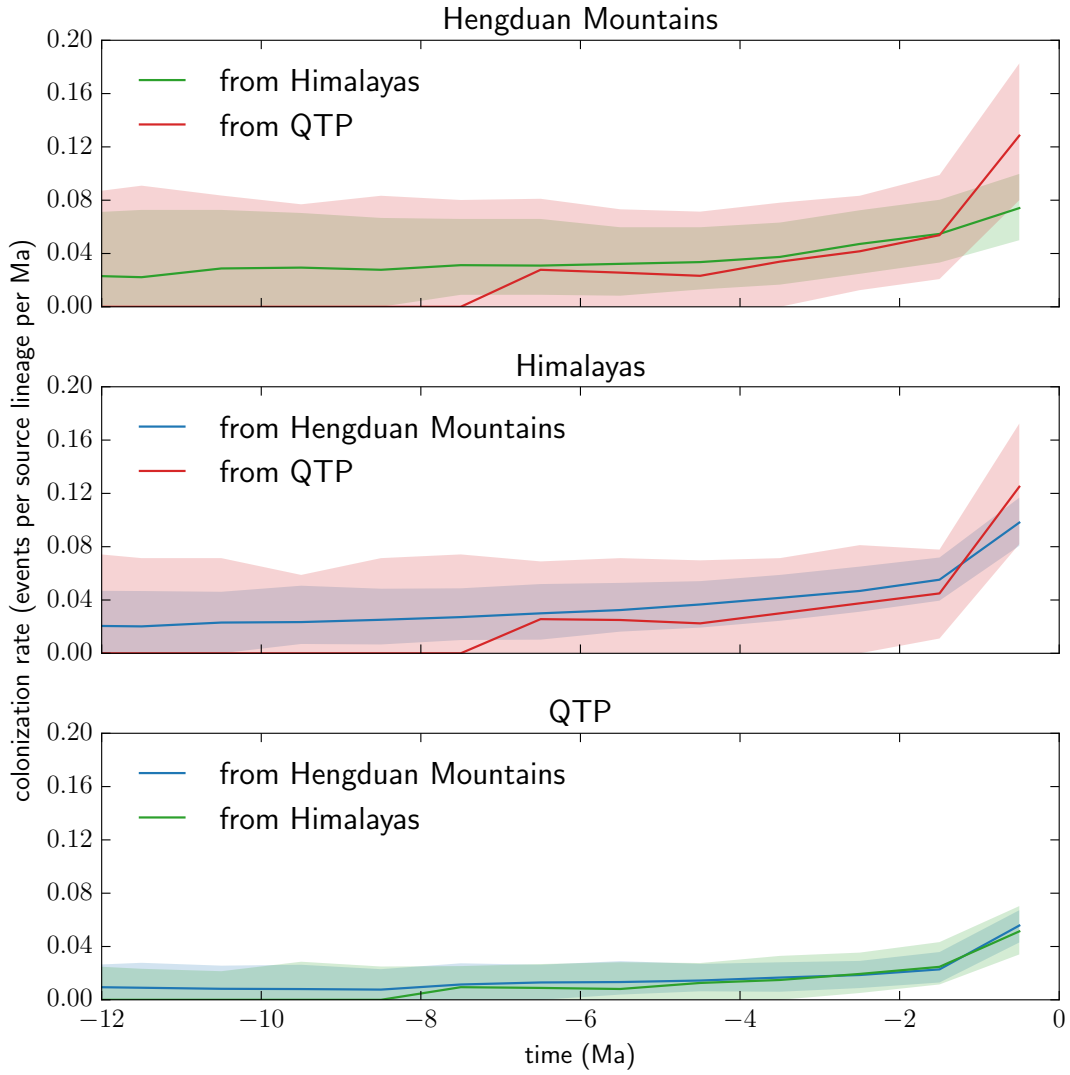


Figure S5: Rolling estimates of colonization rates through time, as described in Figure 4, showing the results from treating the Himalayas and QTP as distinct areas. The dynamics of the Hengduan region are essentially unchanged from the original analysis.

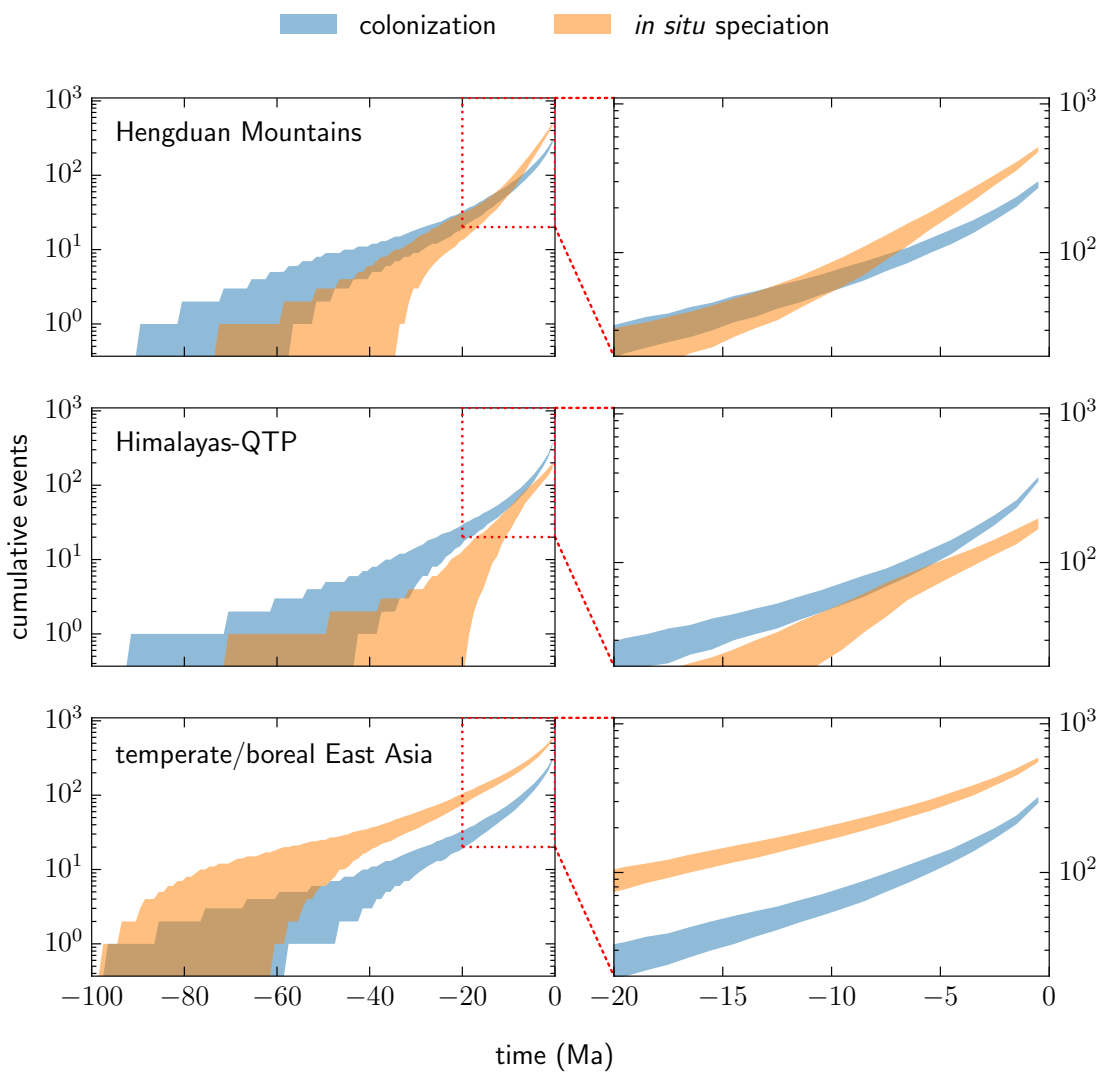


Figure S6: Cumulative numbers of colonization and *in situ* speciation events in 19 plant clades through time, as described in Figure 2. Here, the same analysis is shown, except that is based only on the 17 angiosperm clades. The dynamics of the Hengduan region are essentially unchanged from the original analysis.

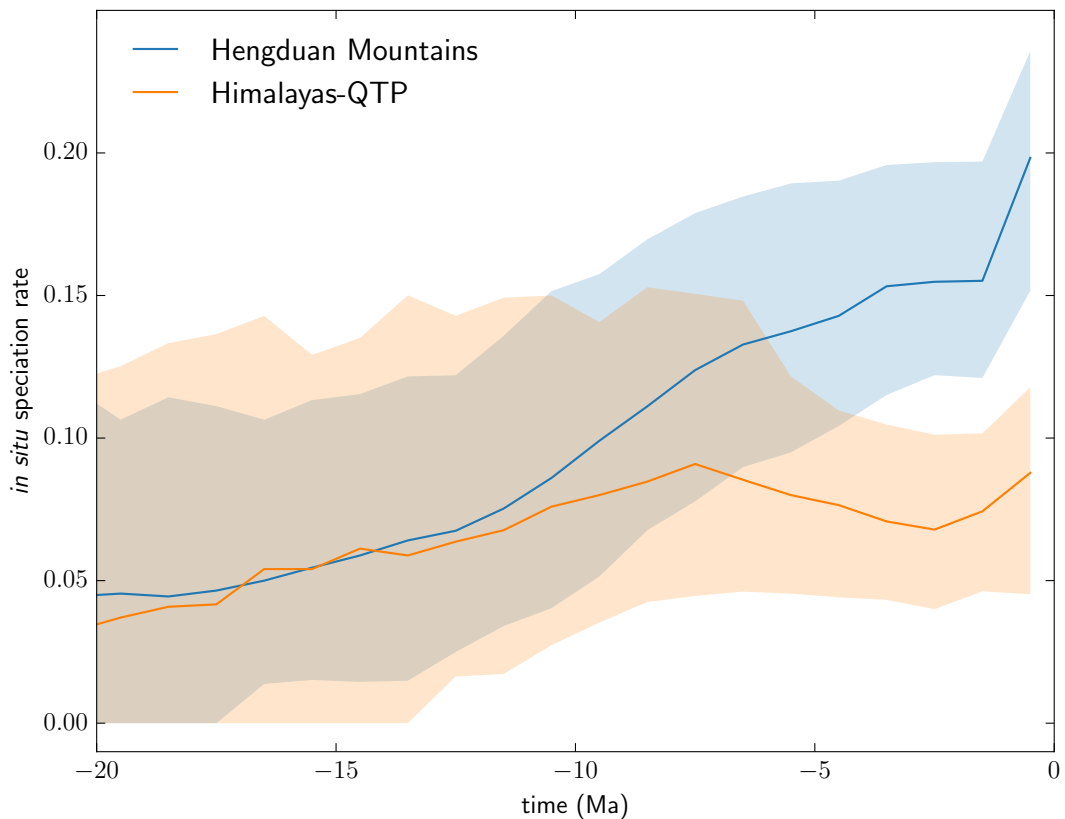


Figure S7: Rolling estimates of *in situ* speciation rates through time, as described in Figure 3. Here, the same analysis is shown, except that is based only on the 17 angiosperm clades. The dynamics of the Hengduan region are essentially unchanged from the original analysis.

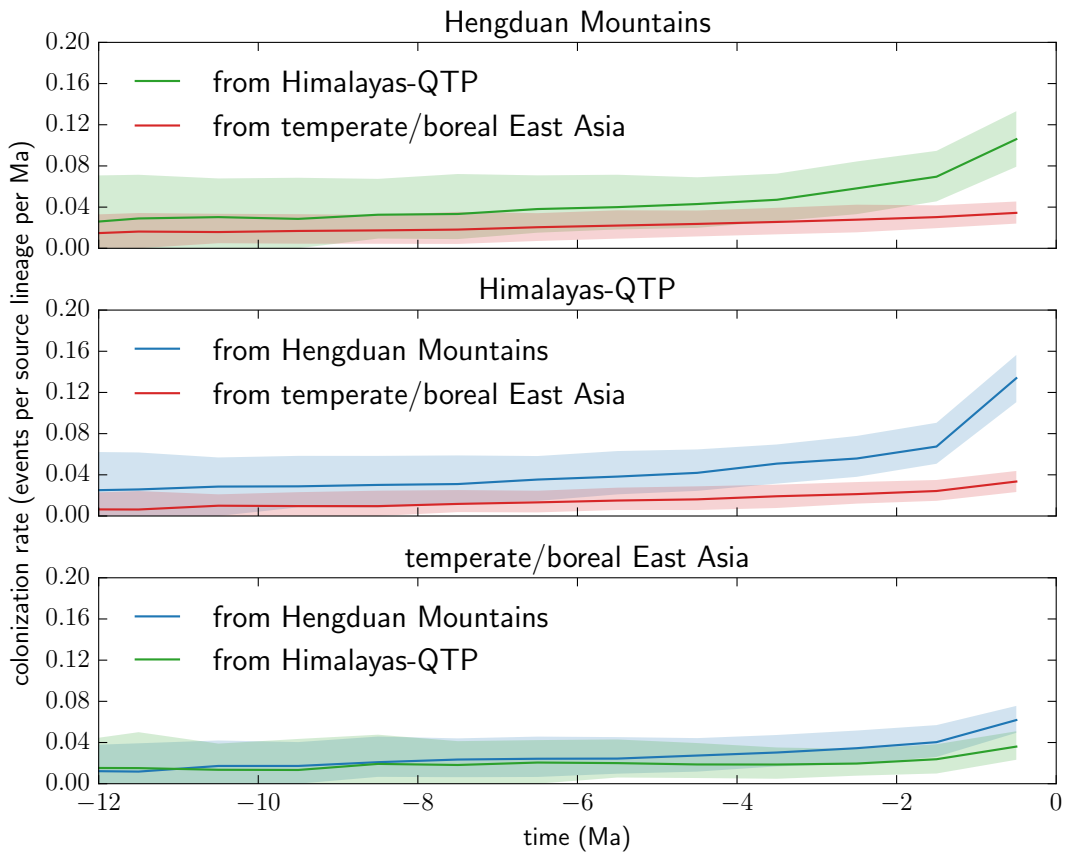


Figure S8: Rolling estimates of colonization rates through time, as described in Figure 4. Here, the same analysis is shown, except that is based only on the 17 angiosperm clades. The dynamics of the Hengduan region are essentially unchanged from the original analysis.

221 **References**

- 222 [1] Alfaro, M.E., Santini, F., Brock, C., Alamillo, H., Dornburg, A., Rabosky, D.L., Carnevale, G. & Harmon, L.J.
223 (2009). Nine exceptional radiations plus high turnover explain species diversity in jawed vertebrates.
224 *Proceedings of the National Academy of Sciences*, 106, 13410–13414.
- 225 [2] Barreda, V., Palazzi, L., Tellería, M., Katinas, L., Crisci, J., Bremer, K., Passalia, M., Corsolini, R., Brizuela,
226 R.R. & Bechis, F. (2010). Eocene Patagonia fossils of the daisy family. *Science*, 329, 1621–1621.
- 227 [3] Barreda, V., Palazzi, L. & Tellería, M.C. (2008). Fossil pollen grains of Asteraceae from the Miocene of
228 Patagonia: Nassauviinae affinity. *Review of Palaeobotany and Palynology*, 151, 51–58.
- 229 [4] Barreda, V.D., Palazzi, L., Katinas, L., Crisci, J.V., Tellería, M.C., Bremer, K., Passala, M.G., Bechis, F. &
230 Corsolini, R. (2012). An extinct Eocene taxon of the daisy family (Asteraceae): evolutionary, ecological and
231 biogeographical implications. *Annals of botany*, 109, 127–134.
- 232 [5] Barreda, V.D., Palazzi, L., Tellería, M.C., Olivero, E.B., Raine, J.I. & Forest, F. (2015). Early evolution of the
233 angiosperm clade Asteraceae in the Cretaceous of Antarctica. *Proceedings of the National Academy of
234 Sciences*, 112, 10989–10994.
- 235 [6] Basinger, J.F. (1976). *Paleorosa similkameenensis*, gen. et sp. nov., permineralized flowers (Rosaceae) from the
236 Eocene of British Columbia. *Canadian Journal of Botany*, 54, 2293–2305.
- 237 [7] Blackmore, S. (1984). The Northwest European Pollen Flora, 32: Compositae-lactuceae. *Review of
238 palaeobotany and palynology*, 42, 45–85.
- 239 [8] Blackmore, S., Van Campo, E. & Crane, P. (1986). Lophate Compositae pollen from the Miocene and Pliocene
240 of the Mediterranean region. *Pollen et spores*, 28, 391–402.
- 241 [9] Bruneau, A., Starr, J.R. & Joly, S. (2007). Phylogenetic relationships in the genus *rosa*: New evidence from
242 chloroplast DNA sequences and an appraisal of current knowledge. *Systematic Botany*, 32, 366–378.
- 243 [10] Van der Burgh, J. (1987). Miocene floras in the lower Rhenish Basin and their ecological interpretation. *Review
244 of Palaeobotany and Palynology*, 52, 299–366.
- 245 [11] Calvillo-Canadell, L. & Cevallos-Ferriz, S.R. (2007). Reproductive structures of Rhamnaceae from the Cerro
246 del Pueblo (Late Cretaceous, Coahuila) and Coatzingo (Oligocene, Puebla) Formations, Mexico. *American
247 Journal of Botany*, 94, 1658–1669.
- 248 [12] Cellinese, N., Smith, S.A., Edwards, E.J., Kim, S.T., Haberle, R.C., Avramakis, M. & Donoghue, M.J. (2009).
249 Historical biogeography of the endemic Campanulaceae of Crete. *Journal of Biogeography*, 36, 1253–1269.

- 250 [13] Chan, K.M.A. & Moore, B.R. (2005). SymmeTREE: whole-tree analysis of differential diversification rates.
251 *Bioinformatics*, 21, 1709–1710.
- 252 [14] Chen, S., Kim, D.K., Chase, M.W. & Kim, J.H. (2013). Networks in a large-scale phylogenetic analysis:
253 reconstructing evolutionary history of Asparagales (Lilianae) based on four plastid genes. *PloS one*, 8, e59472.
- 254 [15] Collinson, M. & Crane, P. (1978). *Rhododendron* seeds from the Palaeocene of southern England. *Botanical
255 Journal of the Linnean Society*, 76, 195–205.
- 256 [16] Collinson, M.E. (1984). *Fossil plants of the London Clay*. Wiley-Blackwell.
- 257 [17] DeVore, M. & Pigg, K. (2007). A brief review of the fossil history of the family Rosaceae with a focus on the
258 Eocene Okanogan Highlands of eastern Washington State, USA, and British Columbia, Canada. *Plant
259 Systematics and Evolution*, 266, 45–57.
- 260 [18] DeVore, M.L., Moore, S.M., Pigg, K.B. & Wehr, W.C. (2004). Fossil *Neviusia* leaves (Rosaceae: Kerrieae)
261 from the lower-middle Eocene of southern British Columbia. *Rhodora*, 106, 197–209.
- 262 [19] Dorofeev, P.I. (1963). *The Tertiary floras of western Siberia*. Moskva, Izd-vo Akademii nauk SSSR, Moscow.
- 263 [20] Fang, M., Fang, R., He, M., Hu, L., Yang, H., Qin, H., Min, T., Chamberlain, D.F., Stevens, P., Wallace, G.D. &
264 Anderberg, A. (2005). Ericaceae. In: *Flora of China* (eds. Wu, Z.Y. & Raven, P.H.). Science Press, Beijing, and
265 Missouri Botanical Garden Press, St. Louis, vol. 14, pp. 242–517.
- 266 [21] Friis, E.M. (1979). The Damgaard flora: a new Middle Miocene flora from Denmark. *Bulletin of the Geological
267 Society of Denmark*, 27, 117–142.
- 268 [22] Friis, E.M., Pedersen, K.R. & Crane, P.R. (2010). Cretaceous diversification of angiosperms in the western part
269 of the Iberian Peninsula. *Review of Palaeobotany and Palynology*, 162, 341–361.
- 270 [23] Gao, Y.D., Harris, A., Zhou, S.D. & He, X.J. (2013). Evolutionary events in *lilium* (including *nomocharis*,
271 Liliaceae) are temporally correlated with orogenies of the Q-T plateau and the Hengduan Mountains. *Molecular
272 Phylogenetics and Evolution*, 68, 443–460.
- 273 [24] Gruas-Cavagnetto, C. (1978). *Étude palynologique de L'Éocène du bassin Anglo-Parisien*. Société géologique
274 de France.
- 275 [25] Hermsen, E.J. (2005). *The fossil record of Iteaceae and Grossulariaceae in the Cretaceous and Tertiary of the
276 United States and Canada*. Thesis, Cornell University.
- 277 [26] Hermsen, E.J. (2013). A review of the fossil record of the genus *Itea* (Iteaceae, Saxifragales) with comments on
278 its historical biogeography. *The Botanical Review*, 79, 1–47.

- 279 [27] Hermsen, E.J., Gandolfo, M.A., Nixon, K.C. & Crepet, W.L. (2003). *Divisestylus* gen. nov.(aff. Iteaceae), a
280 fossil saxifrage from the Late Cretaceous of New Jersey, USA. *American Journal of Botany*, 90, 1373–1388.
- 281 [28] Hochuli, P.A. (1978). Palynologische Untersuchungen im Oligozän und Untermiozän der zentralen und
282 westlichen Paratethys. *Beiträge zur Paläontologie von Österreich*, 4, 1–132.
- 283 [29] Hughes, N.F. (1994). *The enigma of angiosperm origins*. vol. 1. Cambridge University Press.
- 284 [30] Irving, R.S. & Stuessy, T.F. (1971). A new paratropical angiosperm florule in the Eocene Rockdale formation of
285 Bastrop County, Texas. *The Southwestern Naturalist*, pp. 111–116.
- 286 [31] Klymiuk, A.A. & Stockey, R.A. (2012). A Lower Cretaceous (Valanginian) seed cone provides the earliest
287 fossil record for *Picea* (Pinaceae). *American Journal of Botany*, 99, 1069–1082.
- 288 [32] Krutzsch, W. (1970). Die stratigraphisch verwertbaren Sporen-und Pollenformen des mitteleuropäischen
289 Alttertiärs. *Jb. Geol*, 3, 309–379.
- 290 [33] Kvacek, Z. (2001). A new fossil species of *Polypodium* (Polypodiaceae) from the Oligocene of northern
291 Bohemia (Czech Republic). *Feddes Repertorium*, 112, 159–177.
- 292 [34] Lancucka-Srodoniowa, M. (1979). Macroscopic plant remains from the freshwater Miocene of the Nowy Sacz
293 basin (West Carpathians, Poland). *Acta Palaeobotanica*, 20, 3–117.
- 294 [35] Lepage, B. (2003). A new species of *Tsuga* (Pinaceae) from the middle Eocene of Axel Heiberg Island, Canada,
295 and an assessment of the evolution and biogeographical history of the genus. *Botanical Journal of the Linnean
296 Society*, 141, 257–296.
- 297 [36] LePage, B.A. & Basinger, J.F. (1991). A new species of *Larix* (Pinaceae) from the early Tertiary of Axel
298 Heiberg Island, Arctic Canada. *Review of Palaeobotany and Palynology*, 70, 89–111.
- 299 [37] Leslie, A.B., Beaulieu, J.M., Rai, H.S., Crane, P.R., Donoghue, M.J. & Mathews, S. (2012). Hemisphere-scale
300 differences in conifer evolutionary dynamics. *Proceedings of the National Academy of Sciences*, 109,
301 16217–16221.
- 302 [38] Li, Q.Q., Zhou, S.D., He, X.J., Yu, Y., Zhang, Y.C. & Wei, X.Q. (2010). Phylogeny and biogeography of *allium*
303 (Amaryllidaceae: Allieae) based on nuclear ribosomal internal transcribed spacer and chloroplast rps16
304 sequences, focusing on the inclusion of species endemic to China. *Annals of Botany*, 106, 709–733.
- 305 [39] Macphail, M. & Hill, R. (1994). K-Ar dated palynofloras in Tasmania 1: Early Oligocene, Proteacidites
306 tuberculatus Zone sediments, Wilmot Dam, northwestern Tasmania. In: *Papers and Proceedings of the Royal
307 Society of Tasmania*. vol. 128, pp. 1–15.

- 308 [40] Magallón, S., Gómez-Acevedo, S., Sánchez-Reyes, L.L. & Hernández-Hernández, T. (2015). A metacalibrated
309 time-tree documents the early rise of flowering plant phylogenetic diversity. *New Phytologist*, 207, 437–453.
- 310 [41] Mai, D. (1985). Entwicklung der Wasser-und Sumpfplanzen-Gesellschaften Europas von der Kreide bis ins
311 Quartär. *Flora*, 176, 449–511.
- 312 [42] Mai, D. (1995). *Tertiäre Vegetationsgeschichte Mitteleuropas*. Springer, Stuttgart, Heidelberg, New York.
- 313 [43] Mai, H.D. (2001). Die mittelmiozänen und obermiozänen Floren aus der Meuroer und Raunoer Folge in der
314 Lausitz. Teil III: Fundstellen und Paläobiologie. *Palaeontographica Abteilung B*, pp. 1–85.
- 315 [44] Manchester, S.R. (2001). Update on the megafossil flora of Florissant, Colorado. In: *Fossil flora and*
316 *stratigraphy of the Florissant Formation, Colorado* (eds. Evanoff, E., Gregory-Wodzicki, K. & Johnson, K.).
317 Proceedings of the Denver Museum of Nature and Science, pp. 137–161.
- 318 [45] Manchester, S.R. & O’Leary, E.L. (2010). Phylogenetic distribution and identification of fin-winged fruits. *The*
319 *Botanical Review*, 76, 1–82.
- 320 [46] McClain, A.M. & Manchester, S.R. (2001). *Dipteronia* (Sapindaceae) from the Tertiary of North America and
321 implications for the phytogeographic history of the Aceroideae. *American Journal of Botany*, 88, 1316–1325.
- 322 [47] Muller, J. (1981). Fossil pollen records of extant angiosperms. *The Botanical Review*, 47, 1–142.
- 323 [48] Nikitin, V. (2006). *Palaeocarpology and Stratigraphy of the Paleogene and the Neogene Strata in Asian Russia*.
324 Novosibirsk.
- 325 [49] Nixon, K.C. & Crepet, W.L. (1993). Late Cretaceous fossil flowers of ericalean affinity. *American Journal of*
326 *Botany*, pp. 616–623.
- 327 [50] Pigg, K.B. & DeVore, M.L. (2005). *Paleoactaea* gen. nov.(Ranunculaceae) fruits from the Paleogene of North
328 Dakota and the London Clay. *American Journal of Botany*, 92, 1650–1659.
- 329 [51] Pole, M. (1993). Early Miocene flora of the Manuherikia Group, New Zealand. 5. Smilacaceae, Polygonaceae,
330 Elaeocarpaceae. *Journal of the Royal Society of New Zealand*, 23, 289–302.
- 331 [52] Rabosky, D.L. (2007). LASER: A maximum likelihood toolkit for detecting temporal shifts in diversification
332 rates from molecular phylogenies. *Evolutionary Bioinformatics*, 2006.
- 333 [53] Rodríguez de la Rosa, R.A., Cevallos-Ferriz, S.R. & Silva-Pineda, A. (1998). Paleobiological implications of
334 Campanian coprolites. *Palaeogeography, Palaeoclimatology, Palaeoecology*, 142, 231–254.
- 335 [54] Rothwell, G.W., Mapes, G., Stockey, R.A. & Hilton, J. (2012). The seed cone *Eathiestrobus* gen. nov.: fossil
336 evidence for a Jurassic origin of Pinaceae. *American Journal of Botany*, 99, 708–720.

- 337 [55] Schneider, H., Schmidt, A.R., Nascimbene, P.C. & Heinrichs, J. (2015). A new Dominican amber fossil of the
338 derived fern genus *Pleopeltis*. *Organisms Diversity & Evolution*, 15, 277–283.
- 339 [56] Schuettpelz, E. & Pryer, K.M. (2009). Evidence for a Cenozoic radiation of ferns in an angiosperm-dominated
340 canopy. *Proceedings of the National Academy of Sciences*, 106, 11200–11205.
- 341 [57] Schuster, T.M., Setaro, S.D. & Kron, K.A. (2013). Age estimates for the buckwheat family Polygonaceae based
342 on sequence data calibrated by fossils and with a focus on the Amphi-Pacific *Muehlenbeckia*. *PLoS one*, 8,
343 e61261.
- 344 [58] Schwery, O., Onstein, R.E., Bouchenak-Khelladi, Y., Xing, Y., Carter, R.J. & Linder, H.P. (2015). As old as the
345 mountains: the radiations of the Ericaceae. *New Phytologist*, 207, 355–367.
- 346 [59] Soza, V.L., Brunet, J., Liston, A., Salles Smith, P. & Di Stilio, V.S. (2012). Phylogenetic insights into the
347 correlates of dioecy in meadow-rues (*thalictrum*, Ranunculaceae). *Molecular Phylogenetics and Evolution*, 63,
348 180–192.
- 349 [60] Tremetsberger, K., Gemeinholzer, B., Zetsche, H., Blackmore, S., Kilian, N. & Talavera, S. (2013).
350 Divergence time estimation in Cichorieae (Asteraceae) using a fossil-calibrated relaxed molecular clock.
351 *Organisms Diversity & Evolution*, 13, 1–13.
- 352 [61] Vikulin, S. & Bobrov, A. (1987). New fossil genus *Protodynaria* (Polypodiaceae) from the Paleogene flora of
353 Tim (the south of the Middle Russian upland). *Botanicheskii Zhurnal*, 72, 4–31.
- 354 [62] de Vos, J.M., Hughes, C.E., Schneeweiss, G.M., Moore, B.R. & Conti, E. (2014). Heterostyly accelerates
355 diversification via reduced extinction in primroses. *Proceedings of the Royal Society B: Biological Sciences*,
356 281, 20140075.
- 357 [63] Wang, Y.J., Susanna, A., Von Raab-Straube, E., Milne, R. & Liu, J.Q. (2009). Island-like radiation of *saussurea*
358 (Asteraceae: Cardueae) triggered by uplifts of the Qinghai-Tibetan Plateau. *Biological Journal of the Linnean
359 Society*, 97, 893–903.
- 360 [64] Ward, J. & Doyle, J. (1994). Ultrastructure and relationships of mid-Cretaceous polyporate and triporate pollen
361 from northern Gondwana. In: *Ultrastructure of Fossil Spores and Pollen. Its Bearing on Relationships among
362 Fossil and Living Groups* (eds. Kurmann, M. & Doyle, J.). The Royal Botanical Gardens, Kew, pp. 161–172.
- 363 [65] Wen, W.W., Xie, S.P., Liu, K.N., Sun, B.N., Wang, L., Li, H. & Dao, K.Q. (2013). Two species of fern
364 macrofossil from the late Miocene of Lincang, Yunnan, China and their paleoecological implications.
365 *Palaeoworld*, 22, 144–152.

- 366 [66] Weyland, H. (1938). Beiträge zur Kenntnis der rheinischen Tertiärfloren. II. Erste Ergänzungen und
367 Berichtigungen zur Flora der Blätterkohle und des Polierschiefers von Rott im Siebengebirge.
368 *Palaeontographica Abteilung B*, 83, 67–122.
- 369 [67] Wolfe, J.A. & Tanai, T. (1987). Systematics, phylogeny, and distribution of *Acer* (maples) in the Cenozoic of
370 western North America. *Journal of the Faculty of Science, Hokkaido University. Series 4, Geology and*
371 *mineralogy*, 22, 1–246.
- 372 [68] Wu, Y. (2008). *The vascular plants and their eco-geographical distribution of the Qinghai-Tibetan Plateau*.
373 Science Press, Beijing.
- 374 [69] Xiao, W. (2013). *Molecular systematics of Meconopsis Vig. (Papaveraceae): taxonomy, polyploidy evolution,*
375 *and historical biogeography from a phylogenetic insight*. Ph.d. thesis, The University of Texas at Austin.
- 376 [70] Xu, T., Chen, Y., de Jong, P.C., Oterdoom, H.J. & Chang, C.S. (2008). Aceraceae. In: *Flora of China* (eds. Wu,
377 Z.Y. & Raven, P.H.). Science Press, Beijing, and Missouri Botanical Garden Press, St. Louis, vol. 11, pp.
378 515–553.
- 379 [71] Yu, X.Q., Maki, M., Drew, B.T., Paton, A.J., Li, H.W., Zhao, J.L., Conran, J.G. & Li, J. (2014). Phylogeny and
380 historical biogeography of *Isodon* (Lamiaceae): Rapid radiation in south-west China and Miocene overland
381 dispersal into Africa. *Molecular Phylogenetics and Evolution*, 77, 183–194.
- 382 [72] Zhang, D.C., Boufford, D.E., Ree, R.H. & Sun, H. (2009). The 29° N latitudinal line: an important division in
383 the Hengduan mountains, a biodiversity hotspot in southwest China. *Nordic Journal of Botany*, 27, 405–412.